
Electronic Supplementary Material (ESI) for ChemComm.

This journal is © The Royal Society of Chemistry 2019

Electronic Supplementary Information (ESI)

Disulfiram as a potent metallo- β -lactamase inhibitor with dual functional mechanisms

Cheng Chen,^a Ke-Wu Yang,^{*a} Lin-Yu Wu,^b Jia-Qi Li,^a and Le-Yun Sun^a

^aKey Laboratory of Synthetic & Natural Functional Molecule Chemistry of Ministry of Education, Chemical Biology Innovation Laboratory, College of Chemistry & Materials Science, Northwest University, 1 Xuefu Avenue, Xi'an 710127, PR China.

^bCollege of Chemistry and Chemical Engineering, Northwest Normal University, Lanzhou, Gansu 730070, China.

Contents

Experimental Section	2
Inhibitor screening using ITC approach	2
Synthesis of disulfiram analogues and SZn complex	2
Over-expression and purification of M β Ls	4
Determination of IC ₅₀ values	4
Michaelis–Menten kinetics.....	5
ITC experiments.....	5
Zinc displacement analysis by ICP-AES	5
Thermal shift assay	6
Preparation of apo-NDM-1.....	6
The activity restoration of apo-NDM-1.....	7
Construction of the NDM-1 C208A mutant	7
Docking studies.....	7
Screening and identification of NDM-1-producing clinical isolates.....	8
MIC determination	8
Time-dependent kill assay	9
References	9
Supporting Figures.....	10
Supporting Tables	31

Experimental Section

Inhibitor screening using ITC approach

A panel of disulfide compounds (Fig. S1) were screened against purified NDM-1 in combination with 1 mM imipenem. The progress of imipenem hydrolysis by NDM-1 in the presence or absence of different disulfide compounds were monitored using a MicroCal Auto-ITC200 instrument (Malvern Instruments, Malvern, UK) in a single injection mode. Imipenem is rapidly hydrolyzed in the presence of NDM-1 within 10 min, but it is quite slowly and even remain almost unchanged when the inhibitor was added.¹

Synthesis of disulfiram analogues and SZn complex

A mixture of secondary amine (50 mmol), carbon disulfide (51 mmol), potassium hydroxide (110 mmol), and ethanol (250 mL) was heated (50 °C) under stirring for 6 h. To this solution was added 3 g of sodium nitrite in 3 mL of methanol, and under cooling and stirring concentrated HCl (10 mL) was added dropwise. The precipitated product was collected and crystallized from ethanol/methanol to yield 55-65% of the desired compound **3a-e**.^{2,3}

Compound 3a, yellow sticky solid, yield: 56 %, ¹H NMR (400 MHz, Chloroform-*d*): 3.95 – 3.83 (8 H, m), 1.88 – 1.65 (8 H, m), 1.43 – 1.27 (8 H, m), 0.98 – 0.87 (12 H, m). ¹³C NMR (101 MHz, Chloroform-*d*): 193.06, 57.57, 53.38, 30.37, 28.28, 20.22, 13.87. HRMS (ESI): *m/z* Calcd for: C₁₂H₂₀N₂S₄ [M+Na]⁺: 431.1654; found: 431.1653.

Compound 3b, white solid, yield: 65 %, ¹H NMR (400 MHz, DMSO-*d*₆): 4.17 (s, 8 H), 1.65 (d, *J* 21.8, 12 H). ¹³C NMR (101 MHz, Chloroform-*d*): 192.74, 55.86, 52.76, 26.52, 25.65, 24.31. HRMS (ESI): *m/z* Calcd for: C₁₈H₃₆N₂S₄ [M+Na]⁺: 343.0402; found: 343.0400.

Compound 3c, white solid, yield: 75 %, ¹H NMR (400 MHz, DMSO-*d*₆): 3.90 (t, *J* 6.9, 4 H), 3.78 (t, *J* 7.0, 4 H), 2.11 – 2.06 (m, 4 H), 1.99 – 1.89 (m, 4 H). ¹³C NMR (101 MHz, Chloroform-

d): 189.26, 57.08, 51.10, 26.70, 24.36. HRMS (ESI): m/z Calcd for: C₁₀H₁₆N₂S₄ [M+Na]⁺: 315.0089; found: 315.0083.

Compound 3d, grey solid, yield: 53 %, ¹H NMR (400 MHz, Chloroform-*d*) 7.42 – 7.31 (20 H, m), 5.27 (8 H, d, *J* 69.7). ¹³C NMR (101 MHz, Chloroform-*d*): 196.41, 129.27, 128.98, 128.44, 128.03, 127.63, 59.08. HRMS (ESI): m/z Calcd for: C₃₀H₂₈N₂S₄ [M+Na]⁺: 567.1028; found: 567.1039.

Compound 3e, white solid, yield: 63 %, ¹H NMR (400 MHz, DMSO-*d*₆): 4.21 (t, *J* 7.6, 8H), 3.72 (t, *J* 7.9, 8H). ¹³C NMR (101 MHz, Chloroform-*d*): 193.96, 66.51, 53.50. HRMS (ESI): m/z Calcd for: C₁₀H₁₆N₂O₂S₄ [M+Na]⁺: 346.9987; found: 346.9985.

The salicylidene-2-aminothiophenol Schiff base was prepared by a condensation reaction between 1 mol salicylaldehyde with 1 mol o-aminothiophenol in 100 mL ethanol. The ethanolic solution was refluxed for 2 h, cooled to room temperature and the solid Schiff base obtained was filtered, washed three times with alcohol/ether and dried. The Schiff base **NOS** was recrystallized from 50 % acetic acid. yield: 82 %, ¹H NMR (400 MHz, DMSO-*d*₆): 12.59 (s, 1H), 9.03 (s, 1 H), 7.72 (d, *J* 6.8, 1 H), 7.58 (d, *J* 7.2, 1 H), 7.54-7.42 (m, 2 H), 7.36 (t, *J* 7.1, 1 H), 7.29 (t, *J* 7.2, 1 H), 7.02 (t, *J* 6.9, 2 H). ¹³C NMR (101 MHz, DMSO-*d*₆) 164.16, 160.70, 146.51, 134.47, 133.27, 130.89, 128.60, 126.59, 119.95, 119.04, 117.29. HRMS (ESI): m/z Calcd for: C₁₃H₁₁NOS [M+H]⁺: 230.0634; found: 230.0636.

To methanol (15 mL) was added a Schiff base (229 mg, 1.0 mmol) and zinc acetate (220 mg, 1.0 mmol). The mixture solution was refluxed for 15min and then cooled down to ambient temperature. The orange crystalline was filtered off, washed with methanol and **ZnS** complex was obtained after vacuum-dried without further purification,^{4, 5} yield: 90%. ¹H NMR (400 MHz, DMSO-*d*₆): 8.73 (s, 1 H), 7.46 (d, *J* 7.0, 1 H), 7.43 (d, *J* 7.6, 1 H), 7.38 (d, *J* 7.0, 1 H), 7.24 (t, *J* 7.4, 1 H), 6.94-6.97 (m, 2 H), 6.78 (d, *J* 7.9, 1 H), 6.58 (t, *J* 7.0, 1 H). ¹³C NMR (101 MHz, DMSO-*d*₆): 161.90, 145.19, 144.78, 136.13, 133.91, 132.62, 126.62, 122.99,

122.21, 120.69, 116.47, 114.14, 113.84, 49.62. HRMS (ESI): m/z Calcd for: C₁₄H₁₂NO₂SZn [M⁺-31]: 290.9696; found: 290.9710.

Over-expression and purification of MβLs

NDM-1, IMP-1 (B1), ImiS (B2) and L1 (B3) was overexpressed and purified as previously described.⁶ *E. coli* BL21(DE3) cells were first transformed with the over-expression plasmid pET26b-MBLs and the cells were plated on LB-agar plates containing 25 µg/mL kanamycin. A single colony was used to inoculate 50 mL of LB containing 25 µg/mL kanamycin. After preculture overnight at 37 °C, 10 mL cells in LB was used to inoculate 4 × 1 L of LB containing 25 µg/mL kanamycin. The cells were allowed to grow at 37 °C with shaking until the cells reached an OD₆₀₀ of 0.6-0.8. Protein production was induced with 1 mM IPTG, and the cells were shaken at 25 °C for 3~4 h. Then cells were collected by centrifugation (30 min at 8,275 × g) and resuspended in 25 mL of 30 mM Tris, pH 8.0. The cells were lysed by ultrasonication, and the cell debris was separated by centrifugation (30 min at 32,583 × g). The cleared supernatant was dialyzed versus 30 mM Tris, pH 8.0, containing 100 µM ZnCl₂ for 36 h at 4 °C, centrifuged (25 min at 32,583 × g) to remove insoluble matter, and loaded onto an equilibrated Q-Sepharose column. Bound proteins were eluted with a 0-500 mM NaCl gradient in 30 mM Tris, pH 8.0, containing 100 µM ZnCl₂ at 2 mL/min. Fractions (2 mL) containing MBLs were pooled and concentrated with an Amicon ultrafiltration cell equipped with a YM-10 membrane. The crude protein MBLs was run through a G75 column and eluted with 30 mM Tris, pH 8.0, containing 200 mM NaCl. Protein purity was ascertained by SDS PAGE and protein concentration was determined using Beer's law and an extinction coefficient of 27,960 M⁻¹cm⁻¹ for NDM-1, 49,000 M⁻¹cm⁻¹ for IMP-1, 37,250 M⁻¹cm⁻¹ for ImiS and 54,614 M⁻¹cm⁻¹ for L1 at 280 nm.

Determination of IC₅₀ values

The inhibitor concentration causing 50% decrease of enzyme activity (IC₅₀) were determined using imipenem as substrate at room temperature, with 30 mM Tris, pH 7.0. The compounds and substrate concentrations were 0 ~20 µM and 40~60 µM, respectively.

The kinetic values in this study are the means from at least three independent measurements; nine different concentrations of the inhibitor were used to determine the kinetic parameters (IC_{50}) calculated using IC_{50} exe 1.0.0.0 software program.⁷

Michaelis–Menten kinetics

The enzyme (50 nM) was incubated with inhibitor (0 - 2.0 μ M) for 5 h at 298 K with gentle shaking. The final assay buffer contains 30 mM Tris at pH 7.0, with imipenem as the substrate ranging from 10 to 100 μ M. Control experiment was also performed in the absence of inhibitors under the same conditions. The K_m and V_{max} for both the uninhibited and inhibited reactions were obtained by fitting the data into the double reciprocal Lineweaver–Burk plots.⁸

ITC experiments

Isothermal titration calorimetry (ITC) experiments were done on a Malvern MicroCal iTC 200 instrument by a single injection mode.⁹ The purified NDM-1 enzyme and substrate were prepared in 30 mM Tris, pH 7.0, with 5% addition of DMSO. A 30 μ L of imipenem (1 mM) in the syringe was titrated into the sample cell filled with 210 μ L of 10 nM purified NDM-1 protein solution. Heat flow (microcalories/second) was recorded as a function of time. Data were collected every 1 s until the signal returned to the baseline. According to this relationship the rates of substrate hydrolysis are calculated. The NDM-1-catalyzed hydrolysis progress curves of imipenem in the absence and presence of DSF and $Cu(DTC)_2$ are shown in Fig. S7 was obtained by fitting initial velocity versus substrate concentration at each inhibitor concentration using MicroCal Analysis Launcher Origin 7.

Zinc displacement analysis by ICP-AES

The purified NDM-1 sample (10 μ M) dissolved in trace-metal-free buffer containing 50 mM HEPES, pH 7.0, was incubated with various concentrations of DSF and $Cu(DTC)_2$ at 25 °C for 5 h with mild shaking. The sample was subsequently dialyzed in ICP-AES buffer to remove unbound-metal ions and was then acidified and subsequently analyzed using an ICP-AES

spectrometer (Thermo Scientific, IRIS Advantage). Standard calibration curves with correlation coefficients of >0.999 were generated using serial dilutions of metal standards (Zn and Cu). The emission wavelengths used were 213.856 nm (Zn), 324.754 nm (Cu) to ensure the lowest detection limits possible.¹⁰

Thermal shift assay

Thermal shift assay was performed in clear 96-well plates (Invitrogen) using SYPRO Orange (Invitrogen Darmstadt, Germany) as dye. An amount of 4 μ L of test compound (500 μ M final concentration) in assay buffer (50 mM HEPES, pH 7.5, containing 0.01% Triton X-100 for NDM-1) was mixed with 32 μ L of enzyme in assay buffer (final protein concentrations for NDM-1 5 μ M) and 4 μ L of SYPRO Orange ($2.5 \times$ final concentration). Temperature-dependent fluorescence increase reporting protein denaturation was measured in triplicate in an ICycler (Bio-Rad) from 20 to 90 $^{\circ}$ C in steps of 0.2 $^{\circ}$ C at 300 nm excitation and 570 nm emission wavelength. The first derivative of the NDM-1 melting curve was calculated using the Graph Pad software.

Preparation of apo-NDM-1

The apo-NDM-1 was prepared by dialysis against EDTA. Briefly, apo-NDM-1 was derived from the purified NDM-1 obtained above by the two rounds of dialysis against 100 volumes of 10mM Tris-HCl, 200mM NaCl, and 20mM EDTA at pH=7.4 over a 12 h period under stirring. EDTA was removed from the resulting apoenzyme solution by three dialysis steps against 200 volumes of 10mM Tris-HCl, 1M NaCl, pH=7.4, Chelex 100 and finally three dialysis steps against 200 volumes of 50mM Tris-HCl, 200mM NaCl, pH=7.4, and Chelex 100. All buffer solutions used to prepare the apo-enzymes were treated by stirring with Chelex 100 (Bio-Rad). Zinc content in the apoprotein samples was checked using ICP-AES, and apo-NDM-1 contains less than 0.2 molar equivalents of zinc ion.

The activity restoration of apo-NDM-1

The enzyme activities of DSF/Cu(DTC)₂-bound-NDM-1 and apo-NDM-1 were compared upon the supplementation of Zn(II). DSF/Cu(DTC)₂-bound NDM-1 (50 nM) was prepared by pre-incubation of apo-NDM-1 with DSF for 2 h at 25 °C. The above protein solutions were mixed with 0 - 3 molar equivalents ZnSO₄ to NDM-1 and 50 μM imipenem. The change in absorbance at 300 nm was monitored on a UV-visible spectrophotometer at 25 °C for calculation of reaction rates.¹¹

Construction of the NDM-1 C208A mutant

The NDM-1 C208A mutant was constructed as previously described.¹² The wild-type NDM-1-encoding pET26b plasmid was used to introduce C208A mutation by site-directed mutagenesis. The forward primer CGCGTTCGGCGGTGCCCTGATTAAGATAGAAAGC and the reverse was primer was GGCACCGCCGAACGCGAT GTCGGTGCCACAATGCCG. The mutated gene was cloned between the Nde I and Xho I restriction sites into pET-26b harboring a kanamycin resistance gene. The constructed plasmid encoding the C208A mutant were transferred into *E. coli* BL21 (DE3). The expression was determined by SDS-PAGE analysis.

Docking studies

Docking studies of DSF into the active site of NDM-1 (PDB: 4EYL) was performed by AutoDock 4.2. The grid and docking parameter files were prepared using Zn(II) van der Waals parameters = 0.25 kcal/mol and $r^0 = 1.95 \text{ \AA}$. NDM-1 was treated as a rigid receptor. The grid box was centered between the two active-site Zn(II) ions, with dimensions of 60 x 60 x 60 grid points with grid points spaced at 0.375 Å. The mutation rate and crossover rates were set at 0.02 and 0.8, respectively, while the maximum energy evaluations and generations' numbers were set at 2,500,000 and 27,000, respectively. Default values were kept for all other parameter and no constraints were used. Fifty conformations were generated according to the Lamarckian genetic algorithm and grouped into clusters based on a root mean square deviation (RMSD) tolerance of 2.0 Å. The conformations are shown in Fig. S13 are the highest ranked (lowest energy) conformations. Subsequently, the Zn(II) ion

coordinated with Cys208 was removed from the active sites, (diethyl)dithiocarbamate was covalently docked to the active site of NDM-1, based on examples provided by the AutoDock website (<http://autodock.scripps.edu/resources/covalentdocking?searchterm=covalent>), using the flexible residue method.¹³

Screening and identification of NDM-1-producing clinical isolates

Clinical isolate strains were identified and screened by the Phoenix 100 automated bacterial identification system to rapidly detect antimicrobial resistance. Total DNA was extracted by the TIANamp Bacteria DNA Kit according to the manufacturer's protocol. The presence of blaNDM-1 was confirmed using a diagnostic kit for NDM-1 based on fluorescent quantitative polymerase chain reaction assay.

MIC determination

A single colony of *E. coli* BL21 (DH3) expressing NDM-1, IMP-1, ImiS, L1 and clinical isolates *E. coli* producing NDM-1 (from the Health Science Center at Xi'an Jiaotong University, Xian, China) on LB agar plates was transferred to 5 mL of Mueller-Hinton (MH) liquid medium and grown at 37 °C overnight. The bacterial cells were collected by centrifugation (4,000 rpm for 10 min). After discarding the supernatant, the pelleted cells were resuspended in MH medium and diluted to an OD₆₀₀ of 0.5. Bacteria further was diluted to ~10⁵ CFU/mL with MH medium, and then treated with different concentrations of imipenem ranging from 0.03125 to 1024 µg/mL in a series of two-fold dilutions and/or 16 µg/mL inhibitor. Wells with no antibiotics or inhibitors served as growth controls and wells with no bacteria added served as background controls. MIC values were determined by using the Clinical and Laboratory Standards Institute (CLSI) macrodilution (tube) broth method.^{6, 14} The MIC was interpreted as the lowest concentration of the drug that completely inhibited the visible growth of bacteria after incubating plates for 16~18 h at 37 °C. Each inhibitor was tested in triplicate and the highest MIC value was reported.¹⁵ For drug resistance assays, after MICs assay against *E. coli*-NDM-1, withdraw bacterial from the well which contained 1/2 MIC and diluted to 1 × 10⁶ CFU/mL for next MIC measurement. The measurement was repeat for 12 passages.

Time-dependent kill assay

Time kill assay was used to further explore the synergy between imipenem and disulfide compounds. In a typical assay, *E. coli* BL21-NDM-1 was cultured overnight and diluted 1:250 into LB broth at 37 °C for 3 h to reach log phase. The initial bacterial density was adjusted to $\sim 10^7$ CFU/mL and then exposed to imipenem, inhibitor either alone or in combination. LB broth with no drugs served as a control. Aliquots of bacterial suspension were withdrawn at different time intervals (0, 2, 4, 8, 12, 16 and 24 h) for inspection of bacterial viability by agar plating. The concentrations of the drugs used in the test are 16 $\mu\text{g/mL}$ for imipenem, 32 $\mu\text{g/mL}$ for DSF and $\text{Cu}(\text{DTC})_2$. Data from three independent experiments were averaged and plotted as \log_{10} CFU/mL vs. time (h) for each time point over 24 h. All assays were triplicated and performed three times on different days.

References

1. Y. J. Zhang, W. M. Wang, P. Oelschlaeger, C. Chen, J. E. Lei, M. Lv and K. Yang, *ACS Infect Dis*, 2018, **4**, 1671-1678.
2. F. Carta, M. Aggarwal, A. Maresca, A. Scozzafava, R. McKenna, E. Masini and C. T. Supuran, *J. Med. Chem.*, 2012, **55**, 1721-1730.
3. C. N. Kapanda, G. G. Muccioli, G. Labar, J. H. Poupaert and D. M. Lambert, *J. Med. Chem.*, 2009, **52**, 7310-7314.
4. A. L. El-Ansary, A. A. Soliman, O. E. Sherif and J. A. Ezzat, *Synth. React. Inorg. Met.-Org. Chem.*, 2002, **32**, 18.
5. X. Zhang and Y. Chen, *Phys. Chem. Chem. Phys.*, 2012, **14**, 2312-2316.
6. Y. Xiang, C. Chen, W. M. Wang, L. W. Xu, K. W. Yang, P. Oelschlaeger and Y. He, *ACS Med. Chem. Lett.*, 2018, **9**, 359-364.
7. C. Chen, Y. Xiang, K. W. Yang, Y. Zhang, W. M. Wang, J. P. Su, Y. Ge and Y. Liu, *Chem. Commun.*, 2018, **53**, 4802-4805.
8. L. Zhai, Y. L. Zhang, Joon S. Kang, P. Oelschlaeger, L. Xiao, S. S. Nie and K. W. Yang, *ACS Med. Chem. Lett.*, 2016, **7**, 413-417.
9. Y. N. Chang, Y. Xiang, Y. J. Zhang, W. M. Wang, C. Chen, P. Oelschlaeger and K. W. Yang, *ACS Med. Chem. Lett.*, 2017, **8**, 527-532.
10. H. Yang, M. Aitha, A. M. Hetrick, T. K. Richmond, D. L. Tierney and M. W. Crowder, *Biochemistry*, 2012, **51**, 3839-3847.
11. R. Wang, T. P. Lai, P. Gao, H. Zhang, P. L. Ho, P. C. Woo, G. Ma, R. Y. Kao, H. Li and H. Sun, *Nat Commun*, 2018, **9**, 439.
12. T. Pei W, Z. Min, W. Shanshan, G. Hua, L. Dali, X. Dingguo and F. Walter, *Biochemistry*, 2011, **50**, 10102-10113.
13. G. Bianco, S. Forli, D. S. Goodsell, and A. J. Olson. *Protein Science*, 2016, **25**, 295-301.

14. J. M. Andrews, *J. Antimicrob. Chemother.*, 2001, **48**, 5-16.

15. C. Chen, Y Xiang, Y. Liu, X. D. Hu and K. W. Yang. *Med. Chem. Comm*, 2018, **9**, 1172-1177.

Supporting Figures

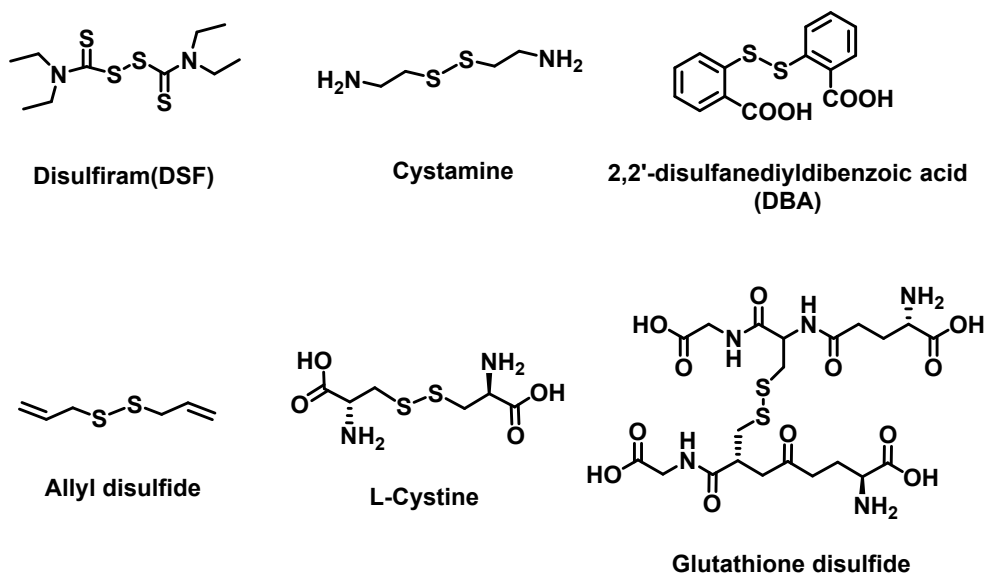


Fig. S1. The structures of disulfide compounds used for initial screening.

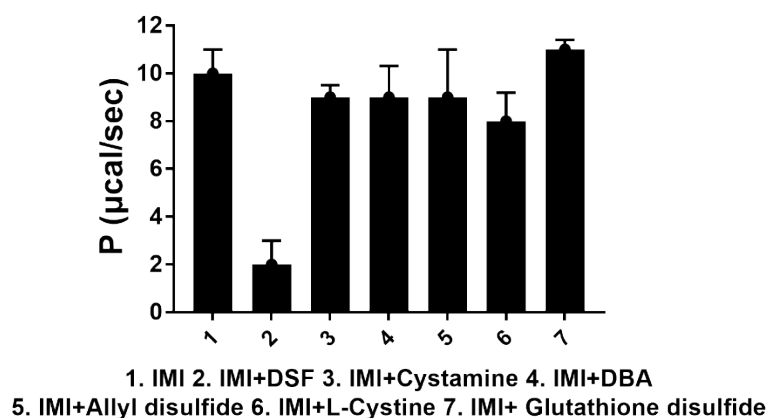


Fig. S2. The heat release of imipenem hydrolysis by the wild-type NDM-1 enzyme in the presence or absence of different disulfide compounds at 100 µM compound concentration by monitoring ITC approach.

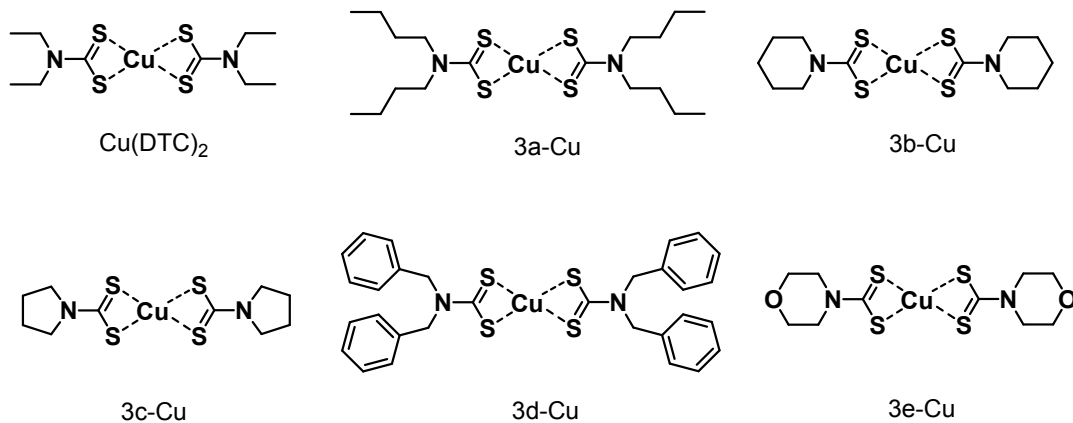


Fig. S4. The structure of $\text{Cu}(\text{DTC})_2$ and its analogues

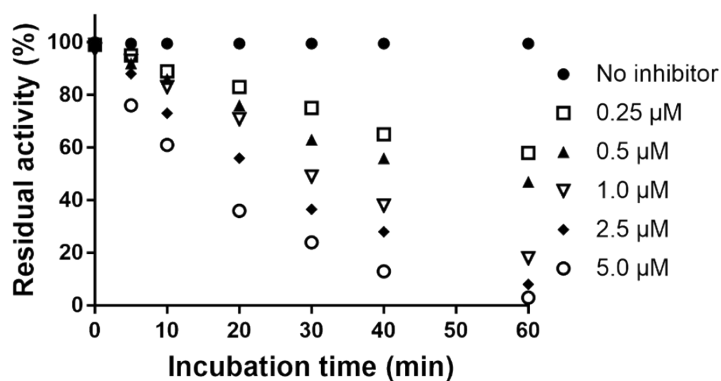


Fig. S5. Time- and concentration-dependent inhibition on NDM-1 by DSF.

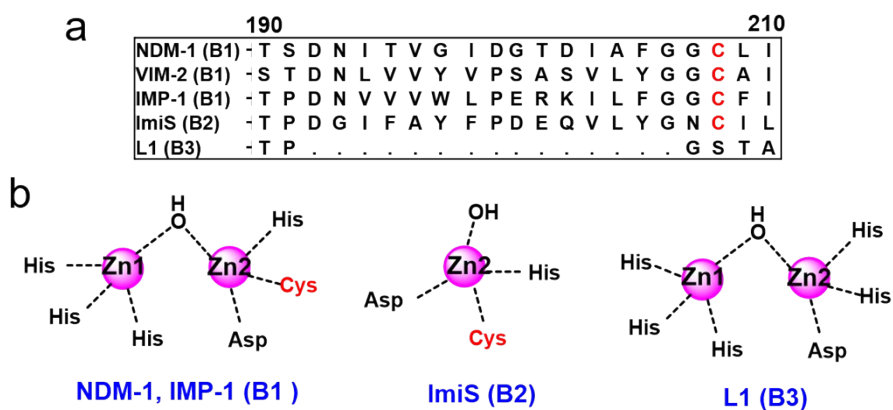


Fig. S6. Comparison of amino acid sequences (a) and the structure of active sites of three different subclasses MβLs (b).

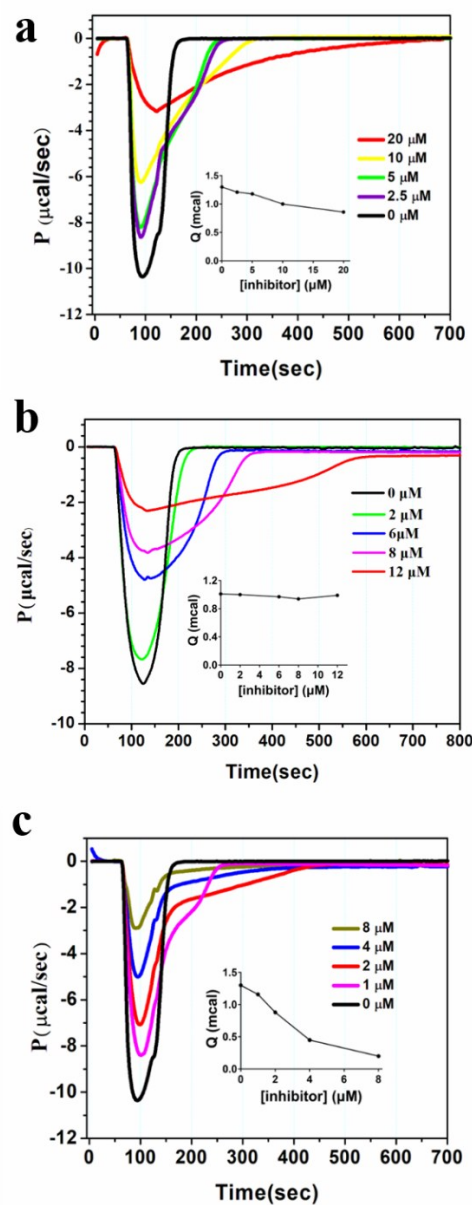


Fig. S7. Overlaid heat flow curves of imipenem hydrolysis with NDM-1 inhibited by DSF (a), CuCl_2 (b) and $\text{Cu}(\text{DTC})_2$ (c).

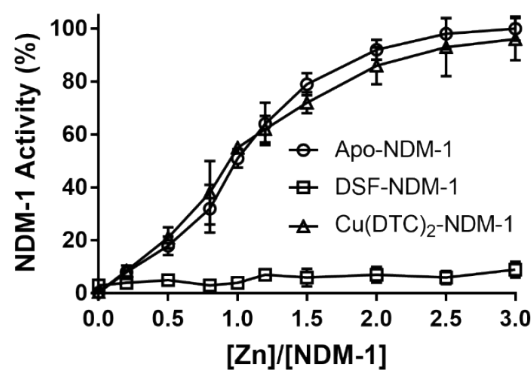


Fig. S8. Activity restoration of NDM-1 upon supplementation of 0 - 3 eq of Zn(II) to 50 nM apo-NDM-1 or DSF/Cu(DTC)₂-NDM-1, addition of 50 μM imipenem, the substrate hydrolysis was monitored at 300 nm on a UV-visible spectrophotometer at 25 °C.

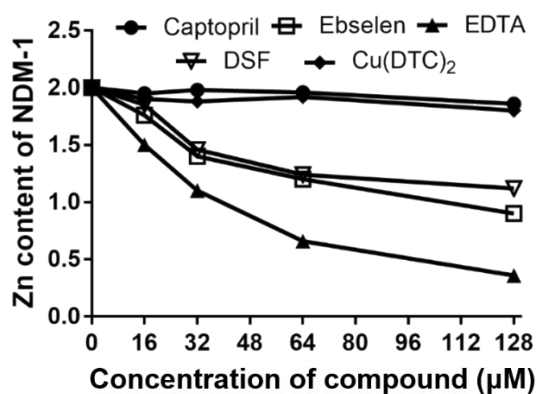


Fig. S9. The release of Zn(II) from 10 μM NDM-1 by 0 - 128 μM captopril, ebselen, EDTA, DSF and Cu(DTC)₂ determined by ICP-AES at 50 mM HEPES, pH 7.0.

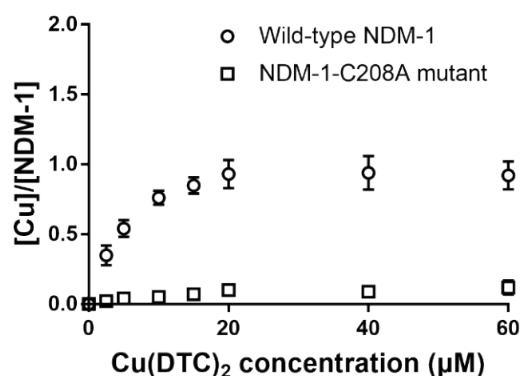


Fig. S10. The Cu content of wild-type NDM-1 and NDM-1-C208A mutant as determined by ICP-AES. The wild-type NDM-1 (20 μM) and NDM-1-C208A mutant (20 μM) incubated with 0 - 60 μM Cu(DTC)₂ for at 5h with 50 mM HEPES, pH 7.0.

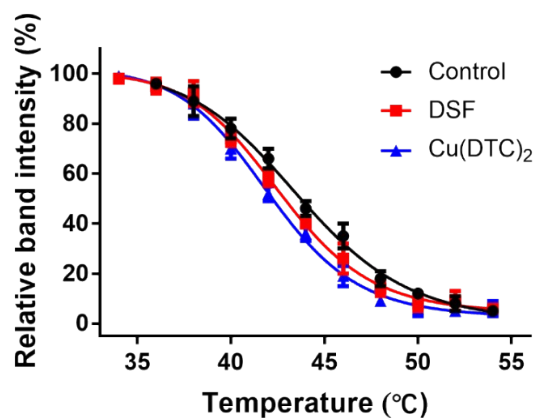


Fig. S11. Thermal shift assays shows that the binding of DSF and Cu(DTC)₂ to NDM-1 shifted the T_m values of NDM-1 from 44.6 to 42.0 and 41.2 °C, respectively.

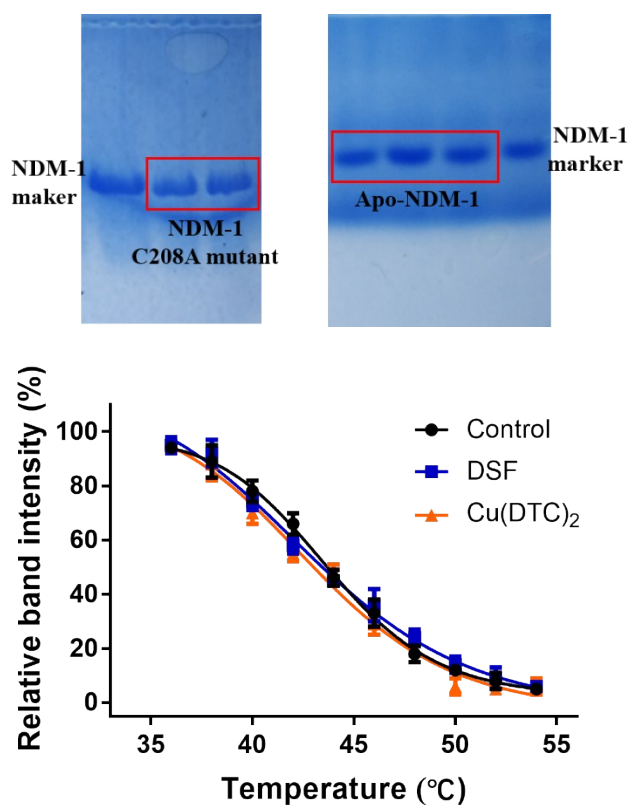


Fig. S12. Original image of SDS-PAGE gel of NDM-1-C208A mutant and apo-NDM-1 (top), no obvious change of corresponding melting temperatures in the C208A-NDM-1 when treated with DSF and Cu(DTC)₂, respectively, compared to the control (bottom).

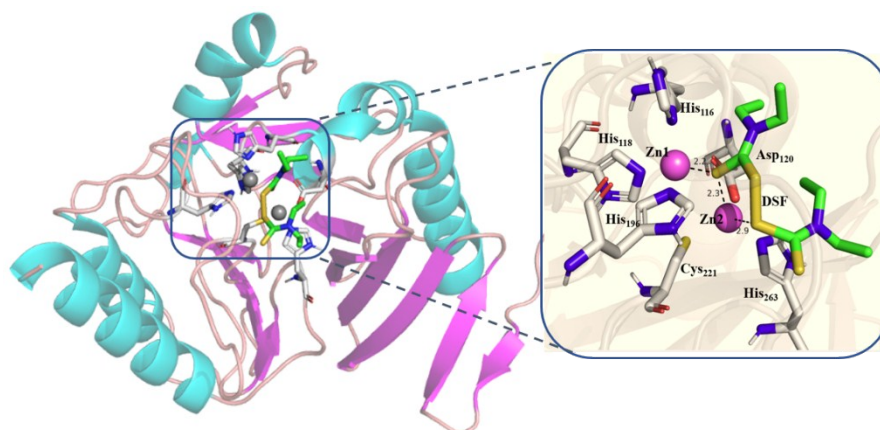


Fig. S13. The binding mode of DSF targeting NDM-1 (PDB: 4EYL). The enzyme backbone is shown as a cartoon in grey, and selected residues are shown as sticks colored by element (H, white; C, cyan; N, blue; O, red; S, yellow). Zn(II) ions are shown as magenta spheres; Characteristic short distances between the inhibitors and the protein are indicated by dashed lines. These figures were generated with PyMOL.

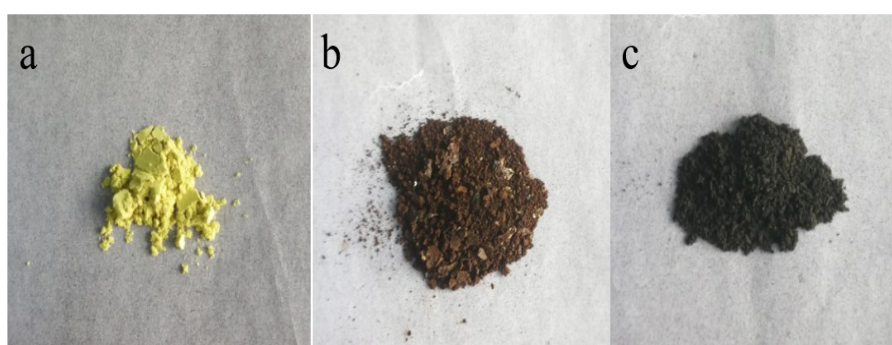


Fig. S14. The color change of SZn complex (a), Cu(DTC)₂ (b), the reaction product of SZn complex and Cu(DTC)₂ (c).

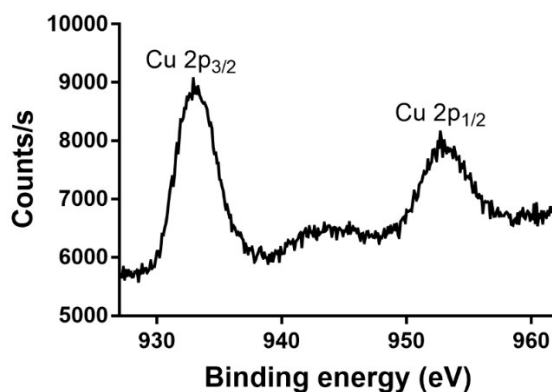


Fig. S15. High-resolution Cu XPS spectrum of Cu(DTC)₂.

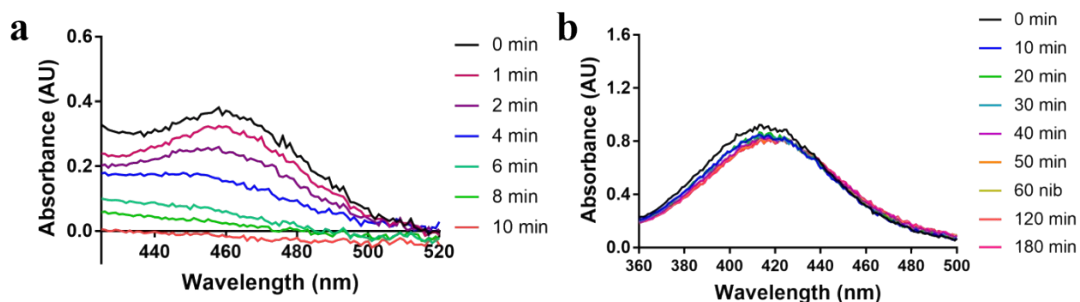


Fig. S16. The reaction between β -mercaptoethanol (β -ME) and CuCl_2 (a) or $\text{Cu}(\text{DTC})_2$ (b) detected by UV-vis spectra at certain time, with CH_3CN as a solvent.

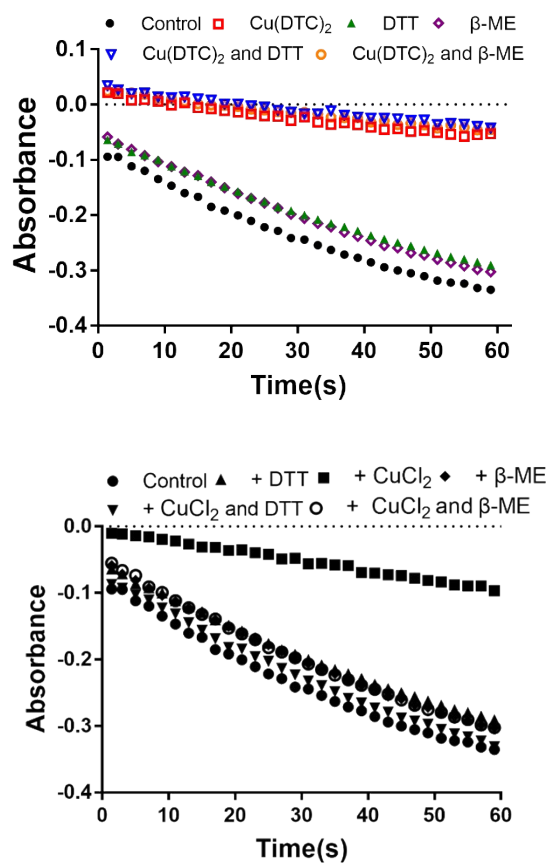


Fig. S17. Effect of dithiothreitol (DTT) and β -mercaptoethanol (β -ME) on the inhibition of NDM-1-catalyzed imipenem hydrolysis by $\text{Cu}(\text{DTC})_2$ (top) and CuCl_2 (bottom).

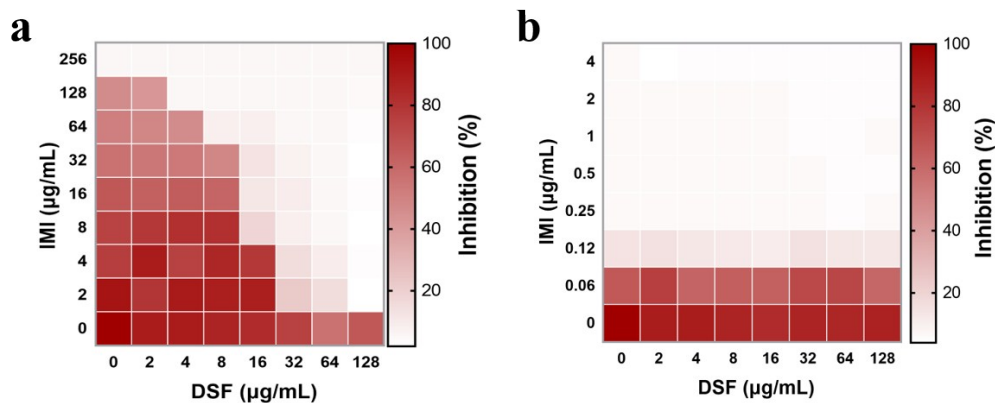


Fig. S18. Representative heat plots of microdilution checkerboard assay for the combination of imipenem (IMI) and DSF against *E. coli*-NDM-1 (a) and *E. coli*-BL21 (b).

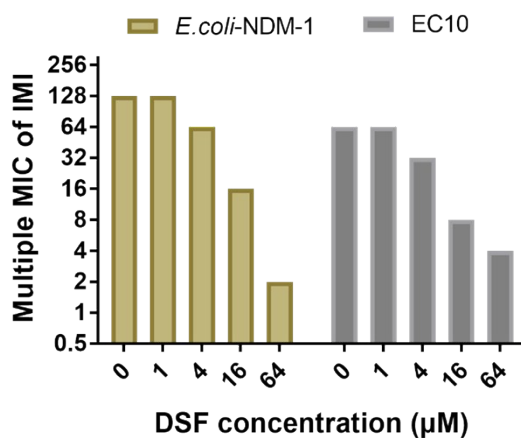


Fig. S19. Multiple in MIC ($\mu\text{g/mL}$) of IMI against *E. coli* expressing NDM-1 and clinical strains producing NDM-1 (EC10) at DSF concentration range of 1–64 $\mu\text{g/mL}$ (c).

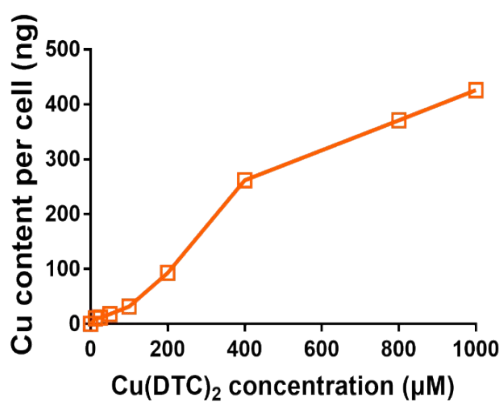


Fig. S20. ICP-AES data for the uptake of copper by *E. coli*-NDM-1 in the absence $\text{Cu}(\text{DTC})_2$.

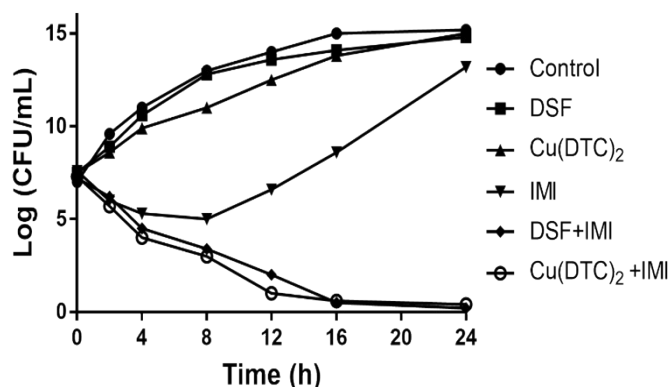


Fig. S21. Time kill curves for IMI and DSF or $\text{Cu}(\text{DTC})_2$ monotherapy and combination therapy against EC10 during 24 h incubation. The concentrations of imipenem (IMI) and inhibitor are 16 $\mu\text{g}/\text{mL}$ and 32 $\mu\text{g}/\text{mL}$, respectively.

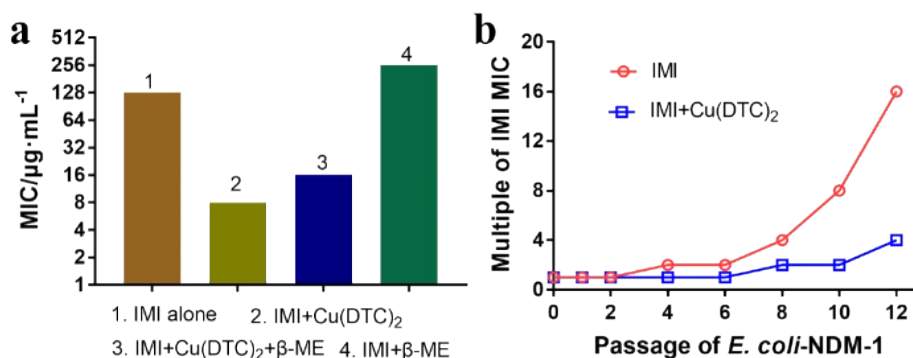


Fig. S22. $\text{Cu}(\text{DTC})_2$ circumvent the reduction by the intracellular thiol (a). Resistance acquisition curves of imipenem or combination of imipenem and $\text{Cu}(\text{DTC})_2$ against *E. coli*-NDM-1 (b).

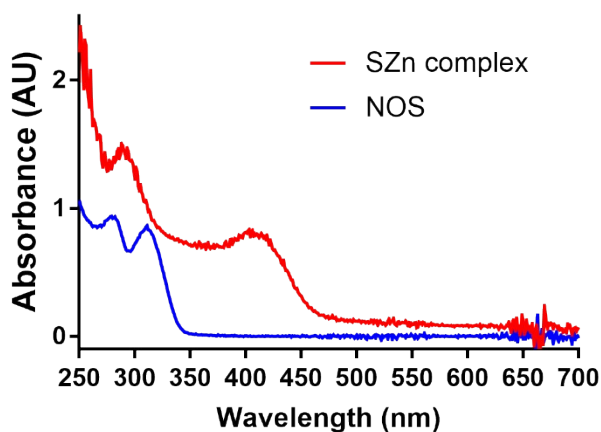


Fig. S23. UV spectrum of NOS and SZn complex, with CH_3CN as a solvent.

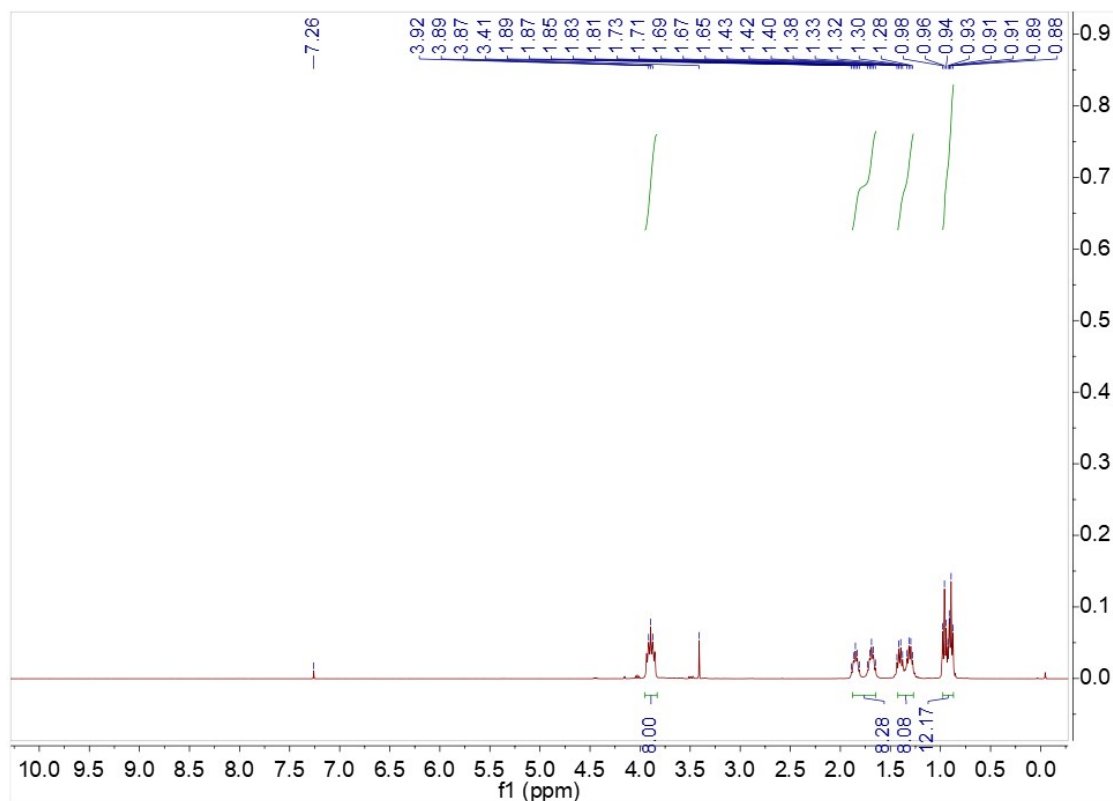


Fig. S24. ¹H NMR spectra of 3a.

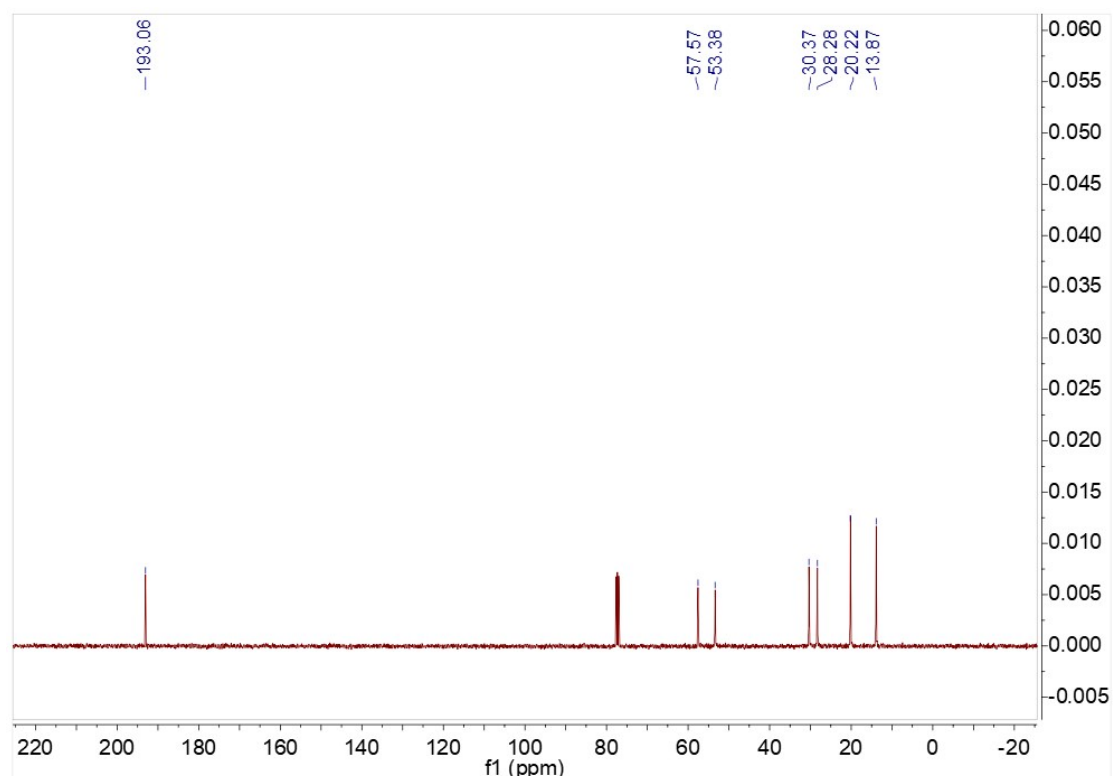


Fig. S25. ¹³C NMR spectra of 3a.

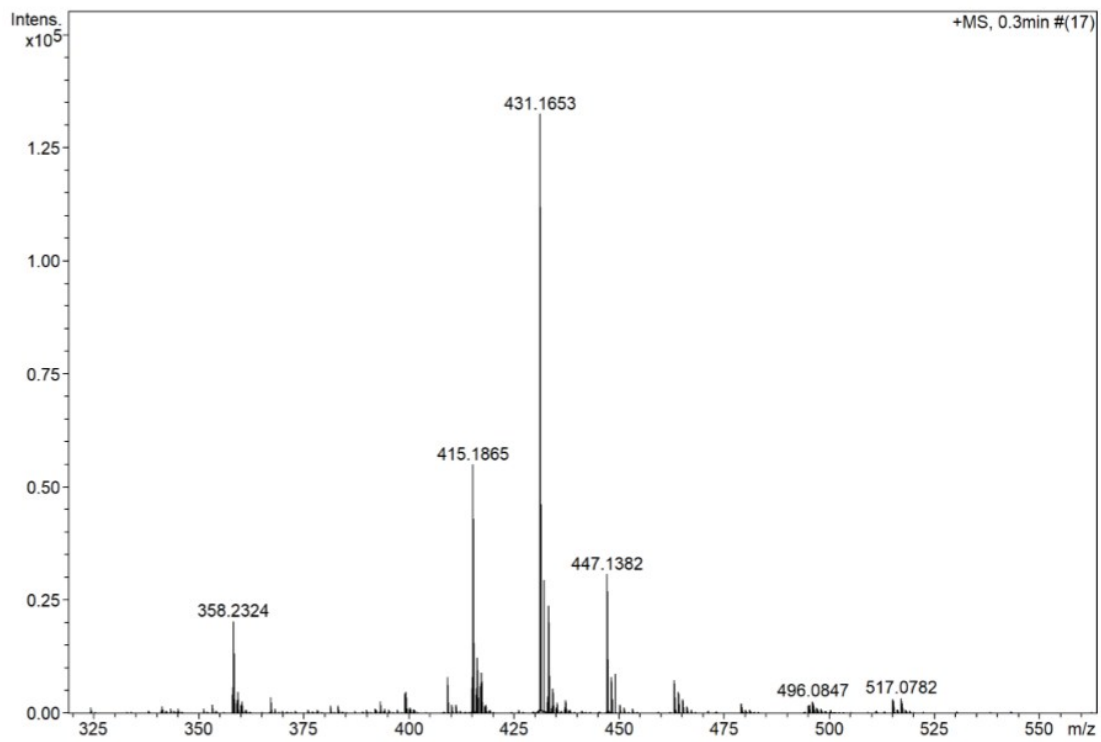


Fig. S26. ESI-MS of 3a.

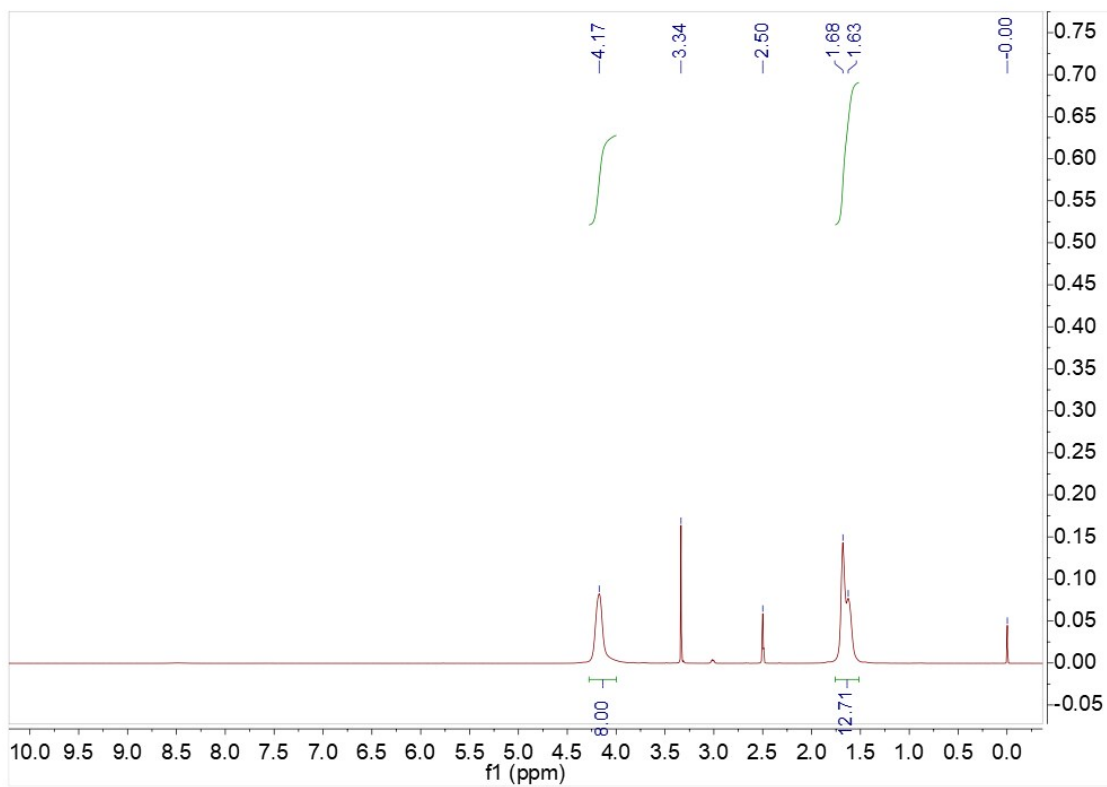


Fig. S27. ^1H NMR spectra of 3b.

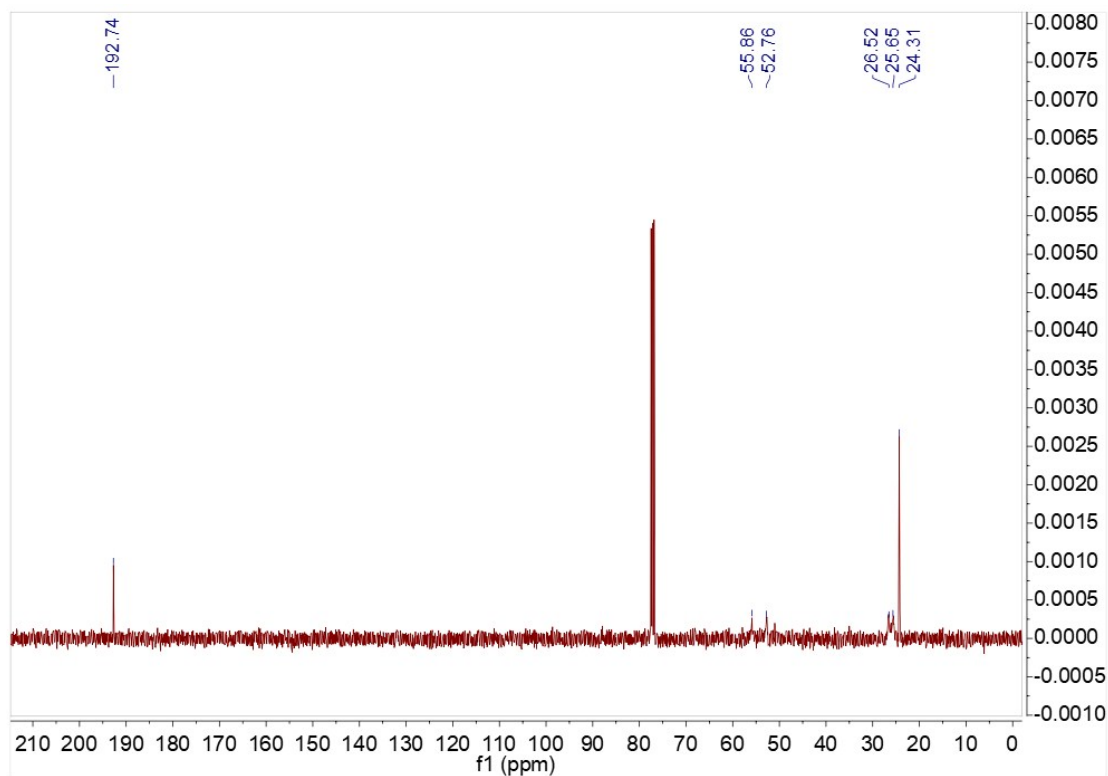


Fig. S28. ¹³C NMR spectra of 3b.

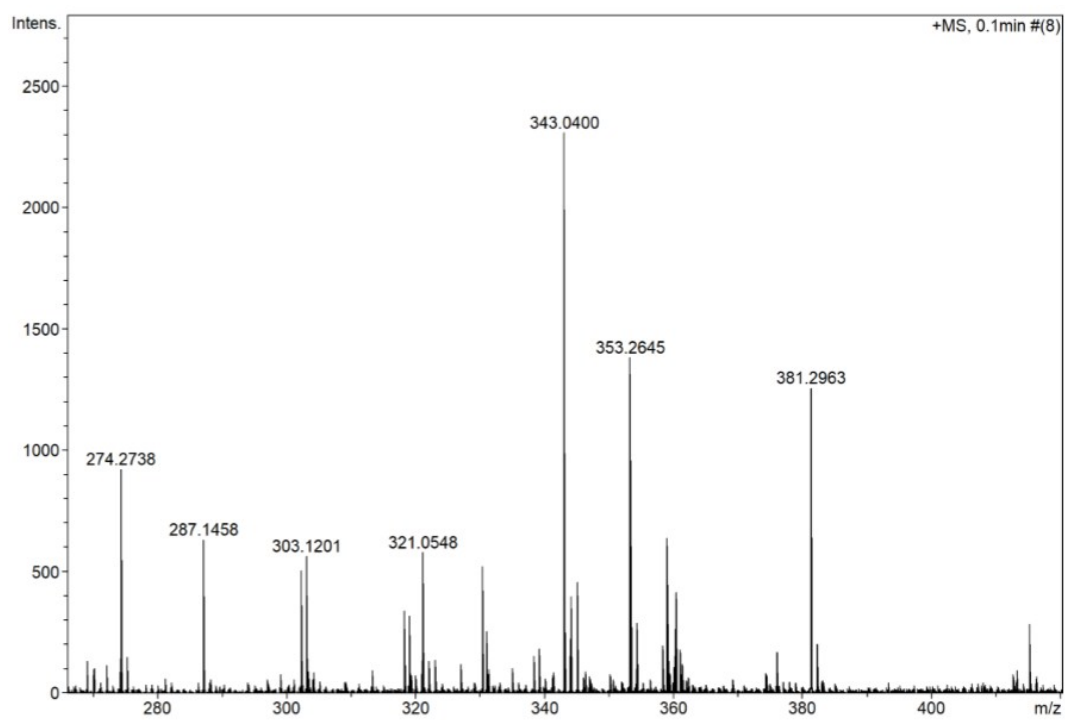


Fig. S29. ESI-MS of 3b.

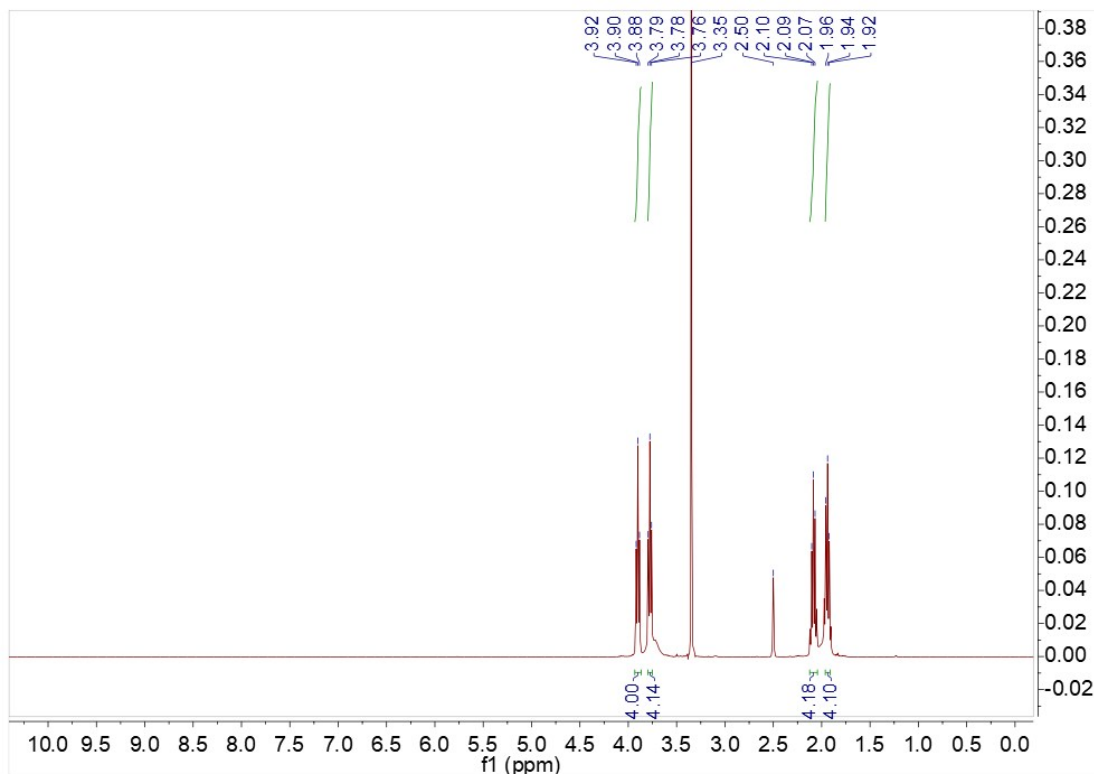


Fig. S30. ^1H NMR spectra of **3c**.

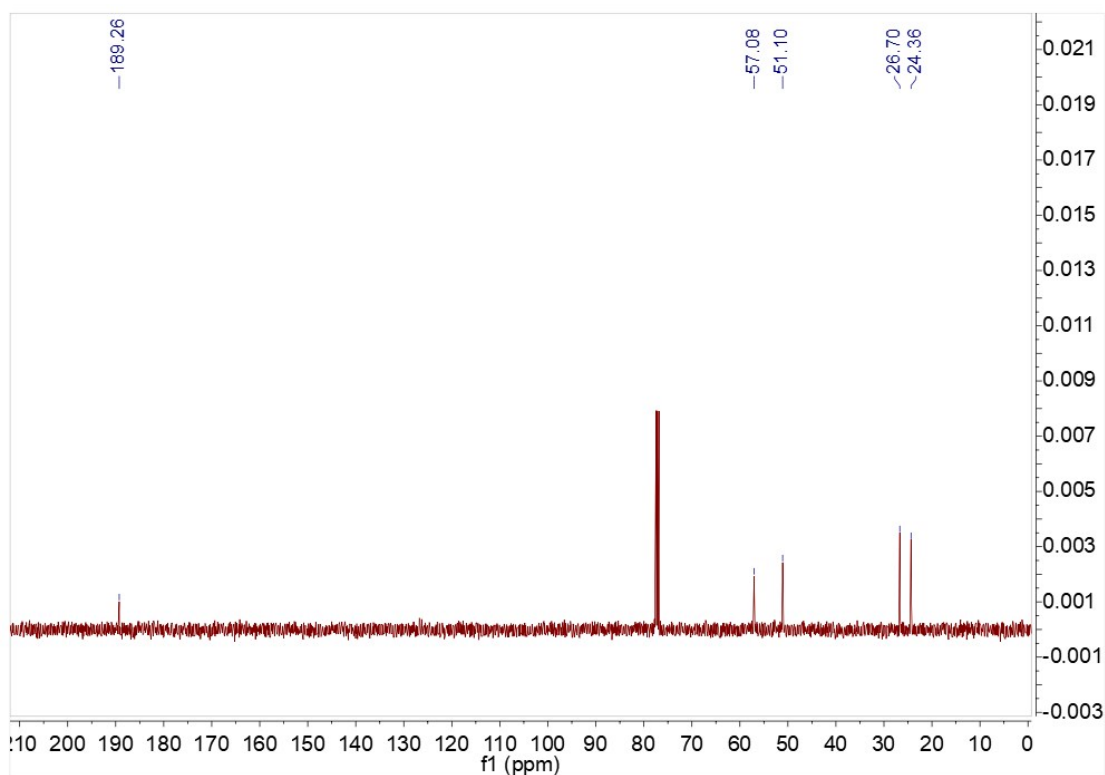


Fig. S31. ^{13}C NMR spectra of **3c**.

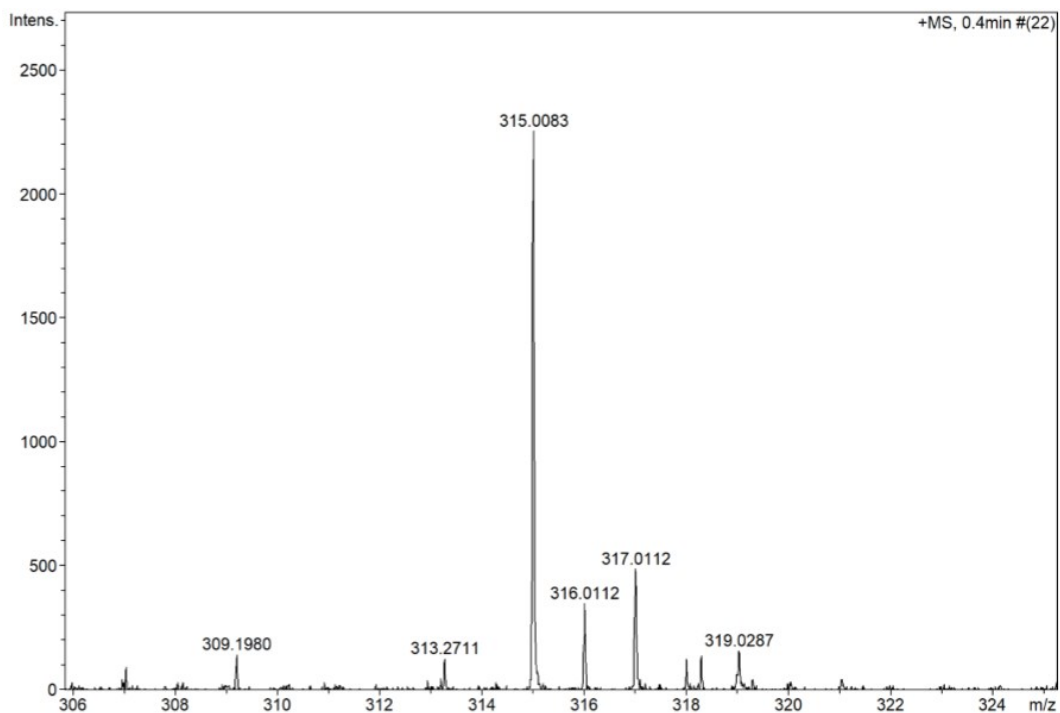


Fig. S32. ESI-MS of 3c.

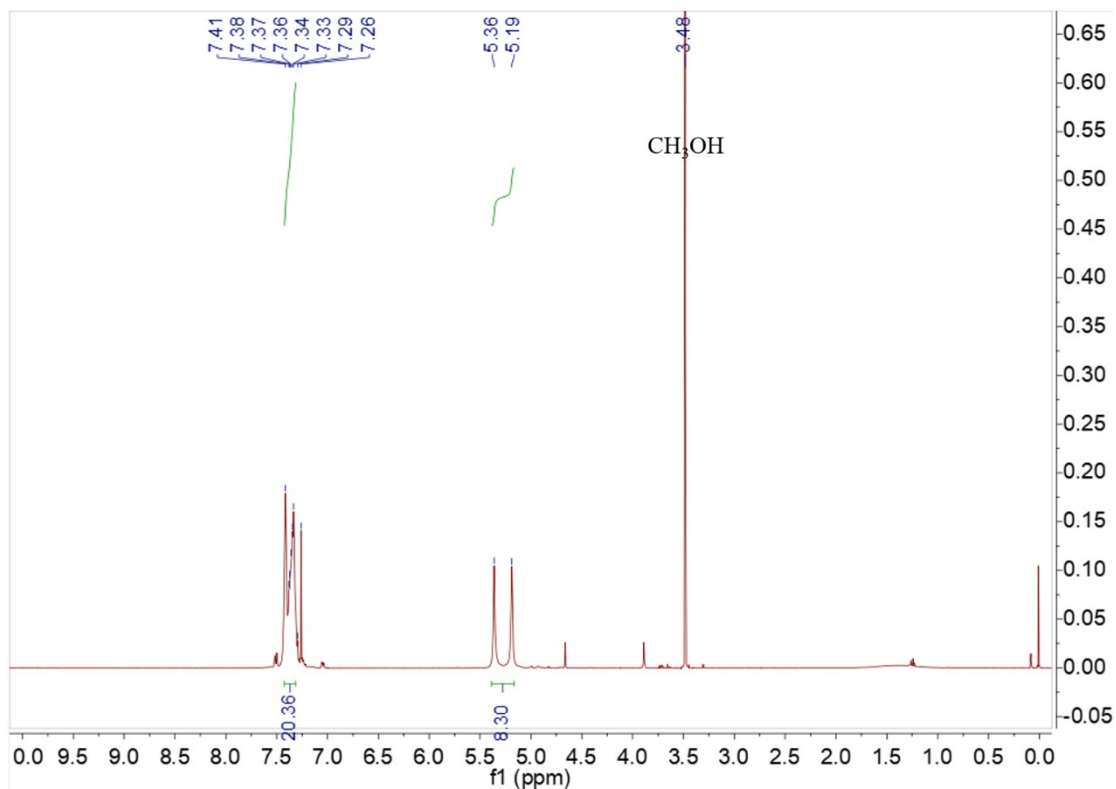


Fig. S33. ¹H NMR spectra of 3d.

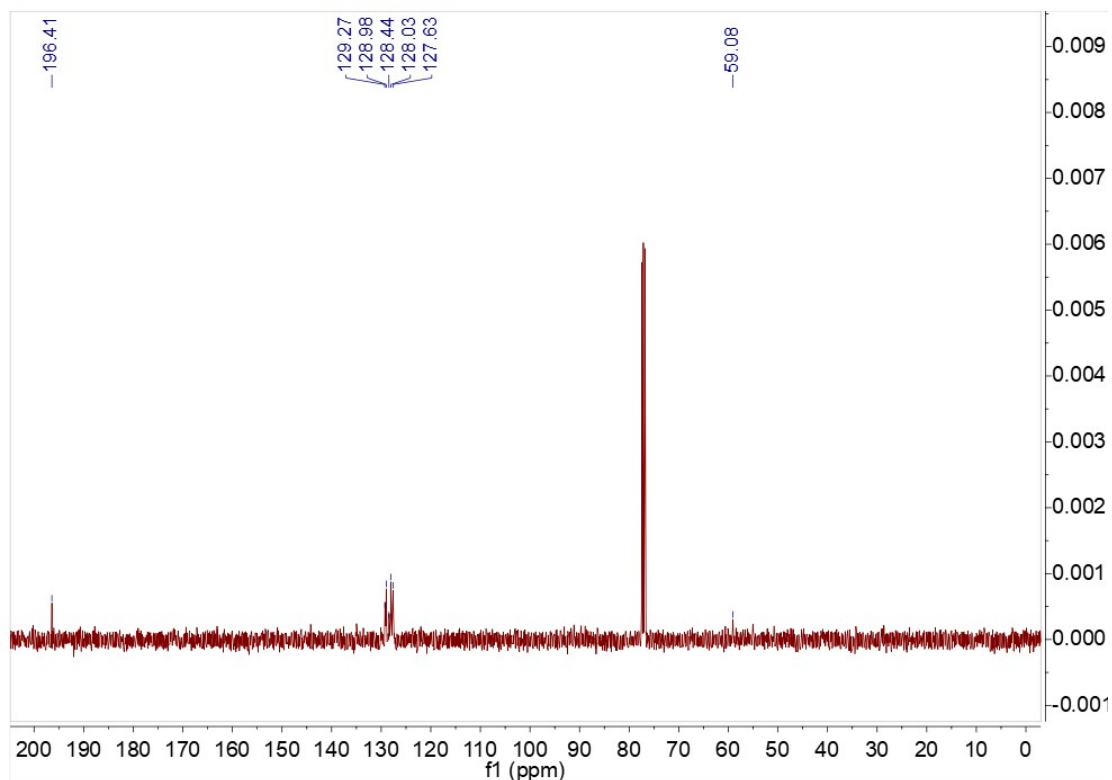


Fig. S34. ^{13}C NMR spectra of 3d.

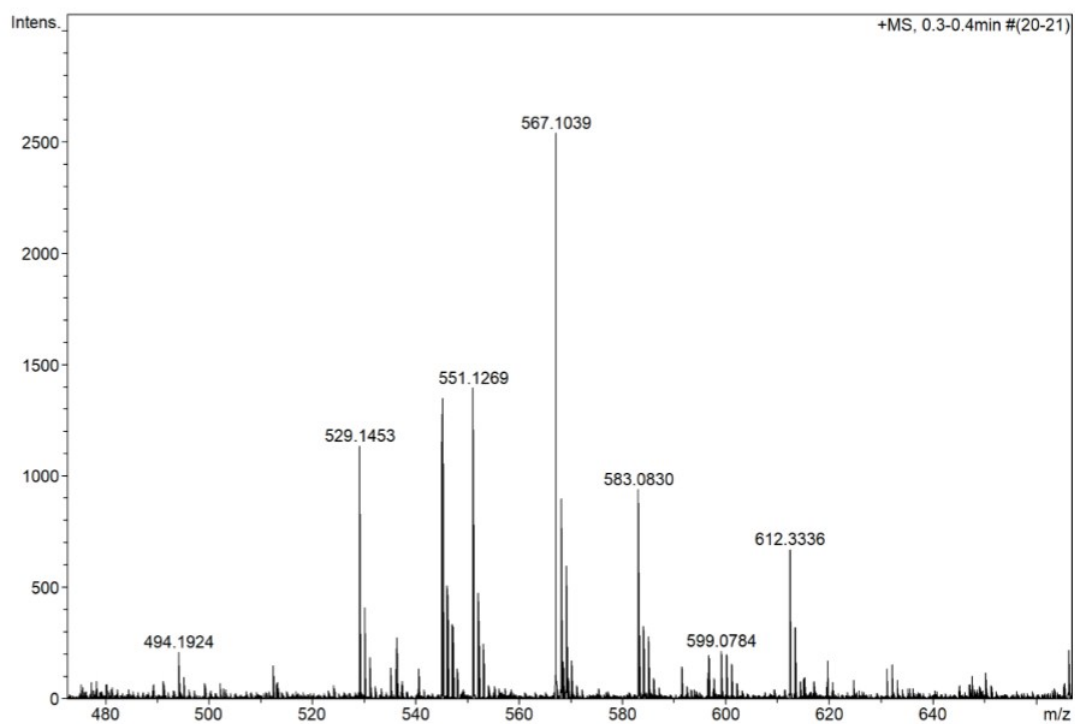


Fig. S35. ESI-MS of 3d.

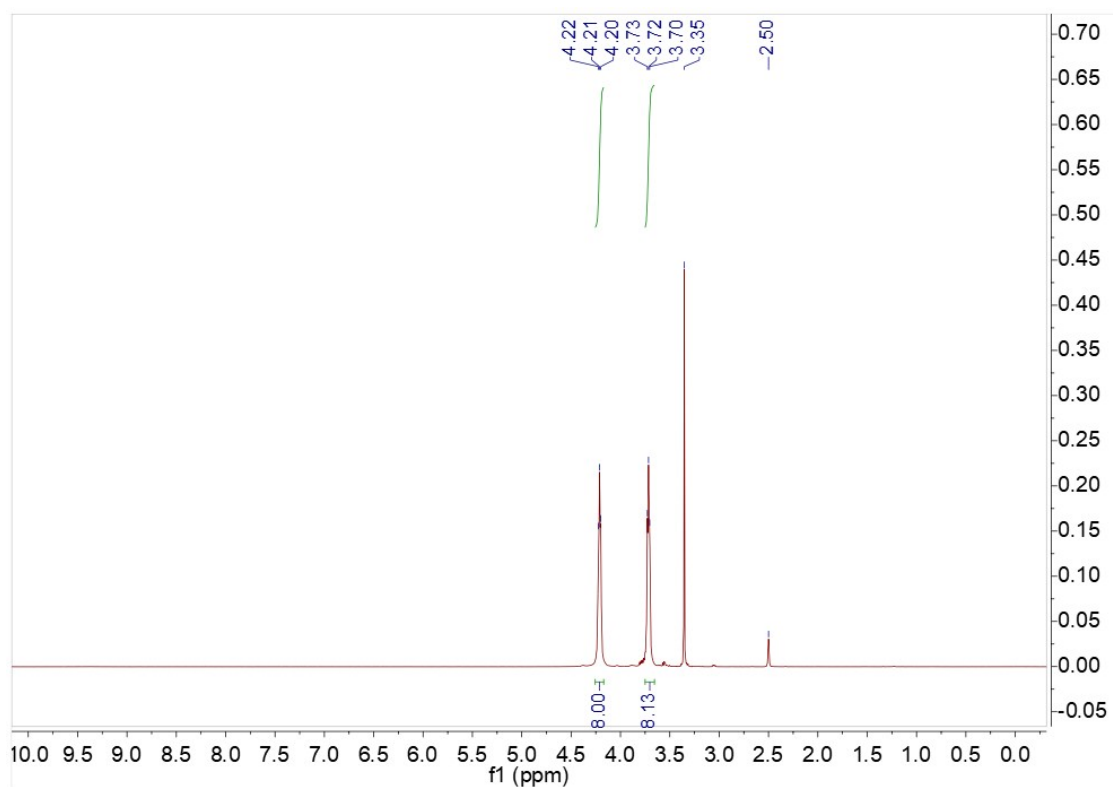


Fig. S36. ^1H NMR spectra of **3e**.

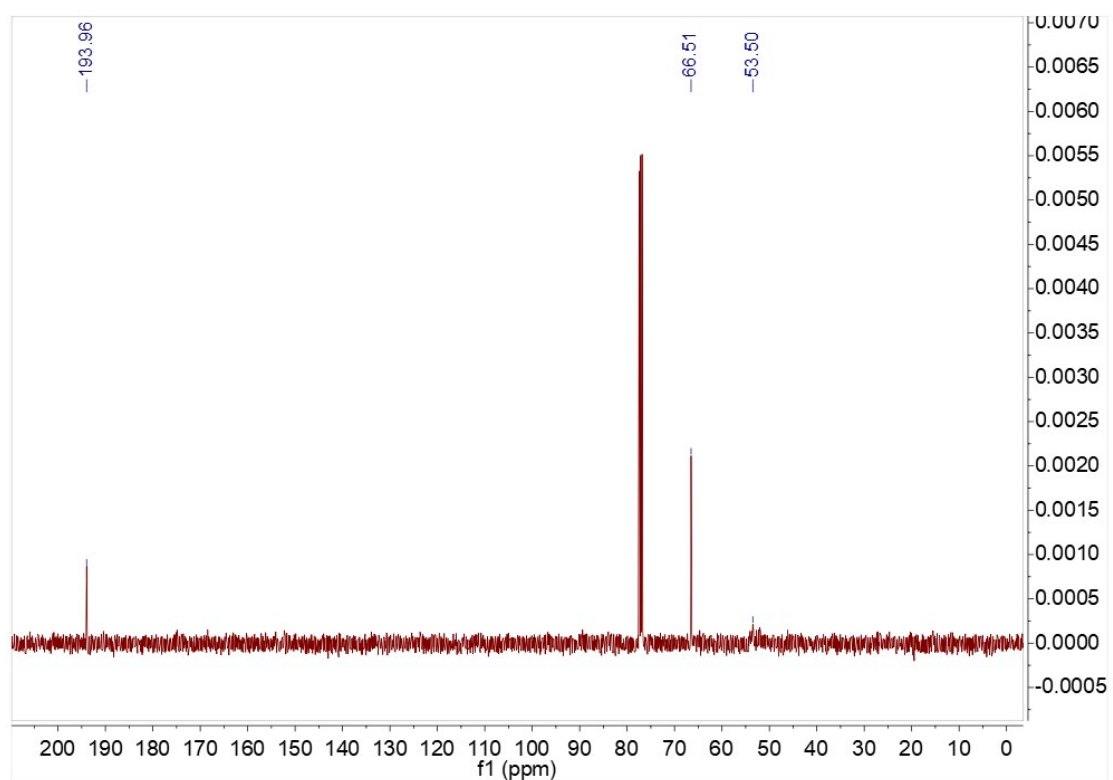


Fig. S37. ^{13}C NMR spectra of **3e**.

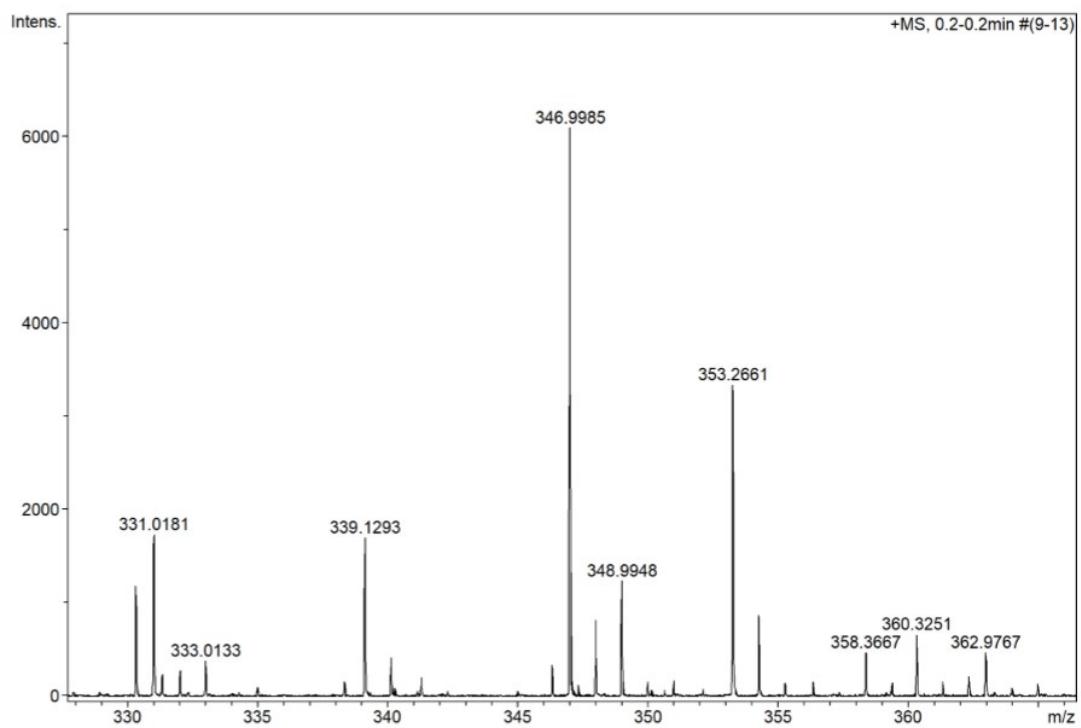


Fig. S38. ESI-MS of 3e.

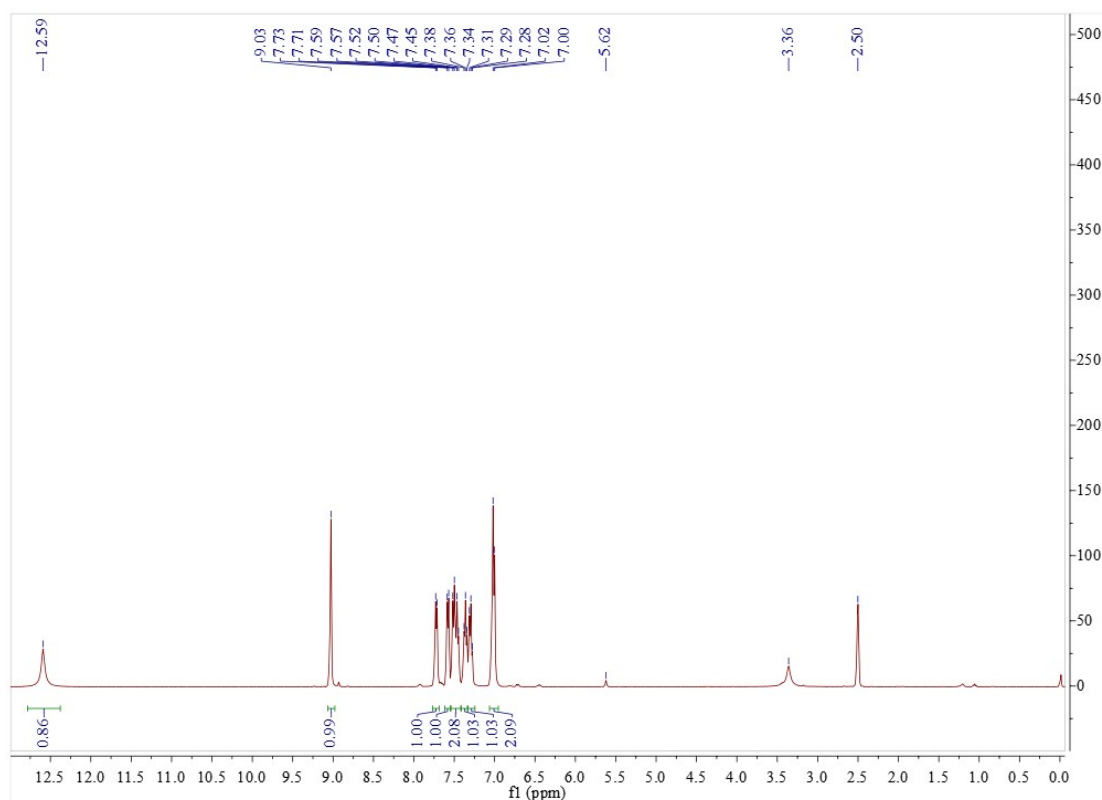


Fig. S39. ¹H NMR spectra of NOS.

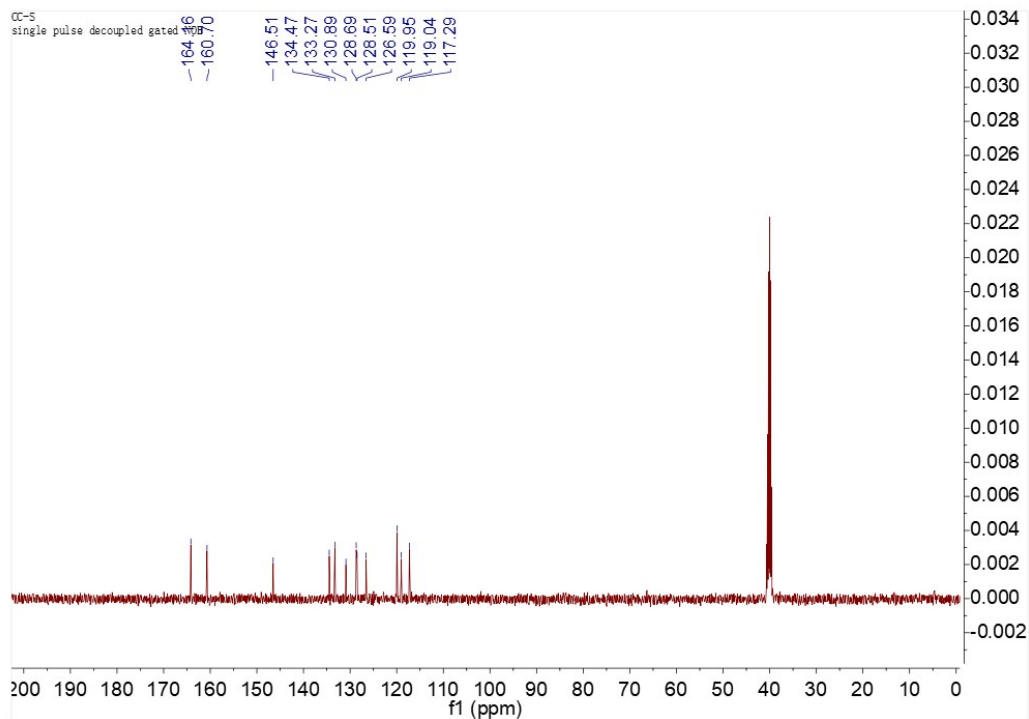


Fig. S40. ¹³C NMR spectra of NOS.

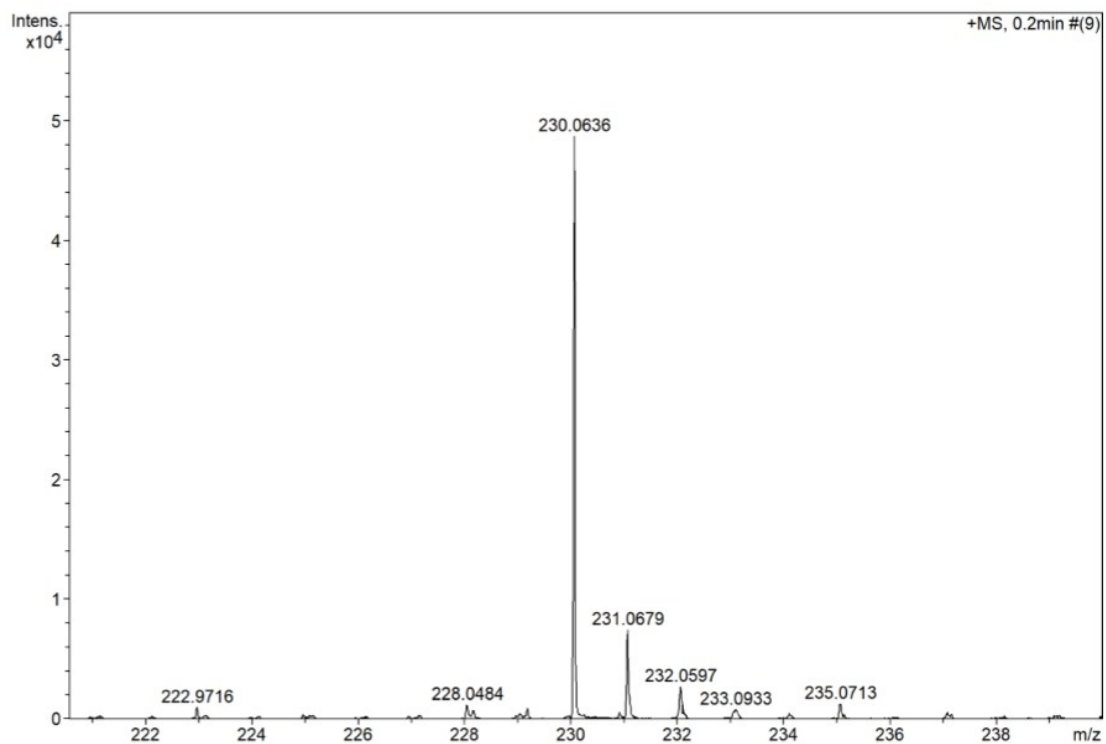


Fig. S41. ESI-MS of NOS.

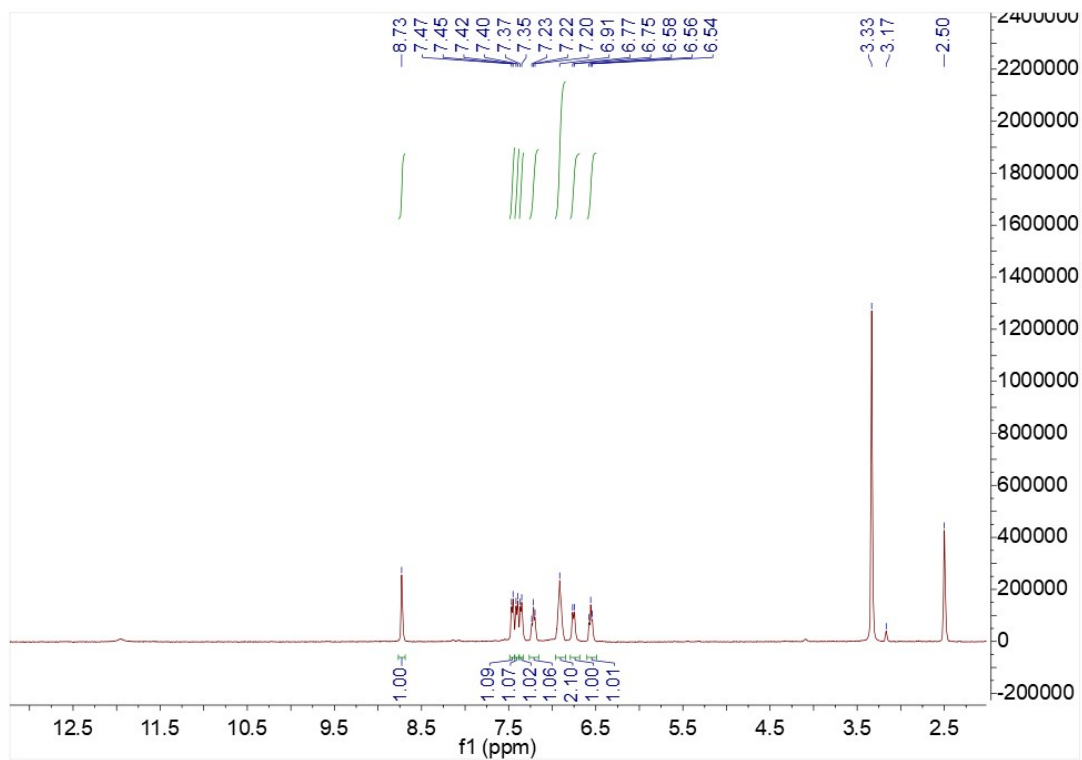


Fig. S42. ¹H NMR spectra of SZn.

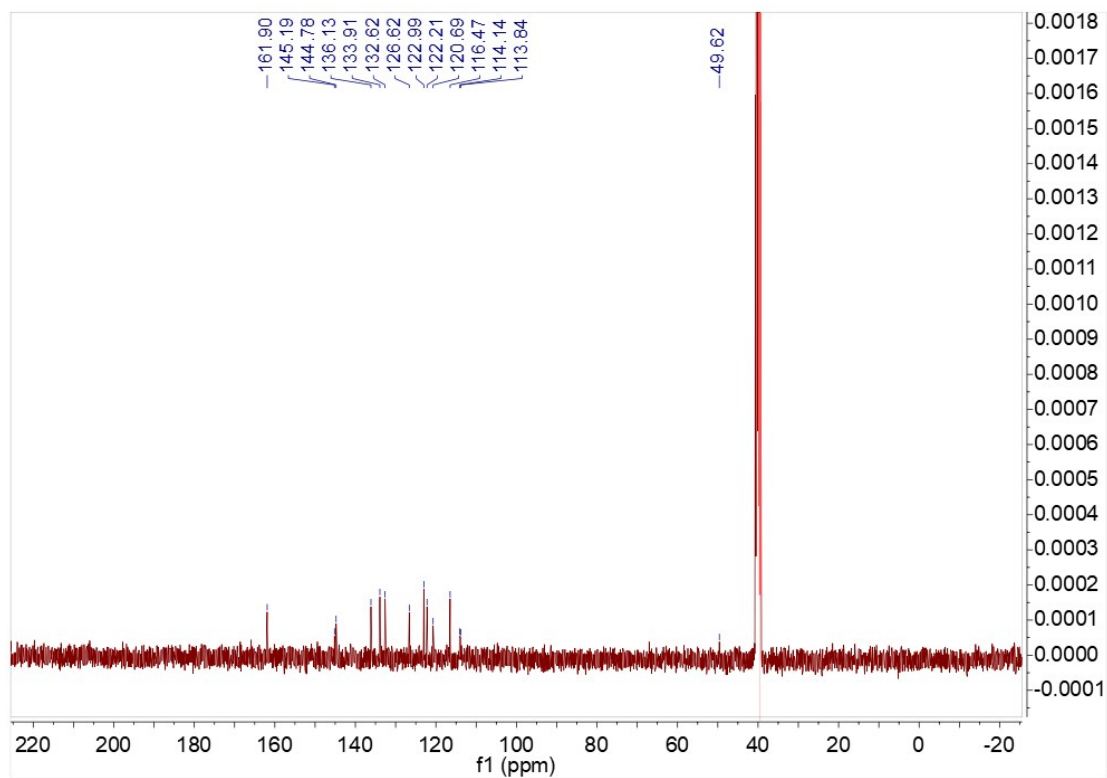


Fig. S43. ¹³C NMR spectra of SZn.

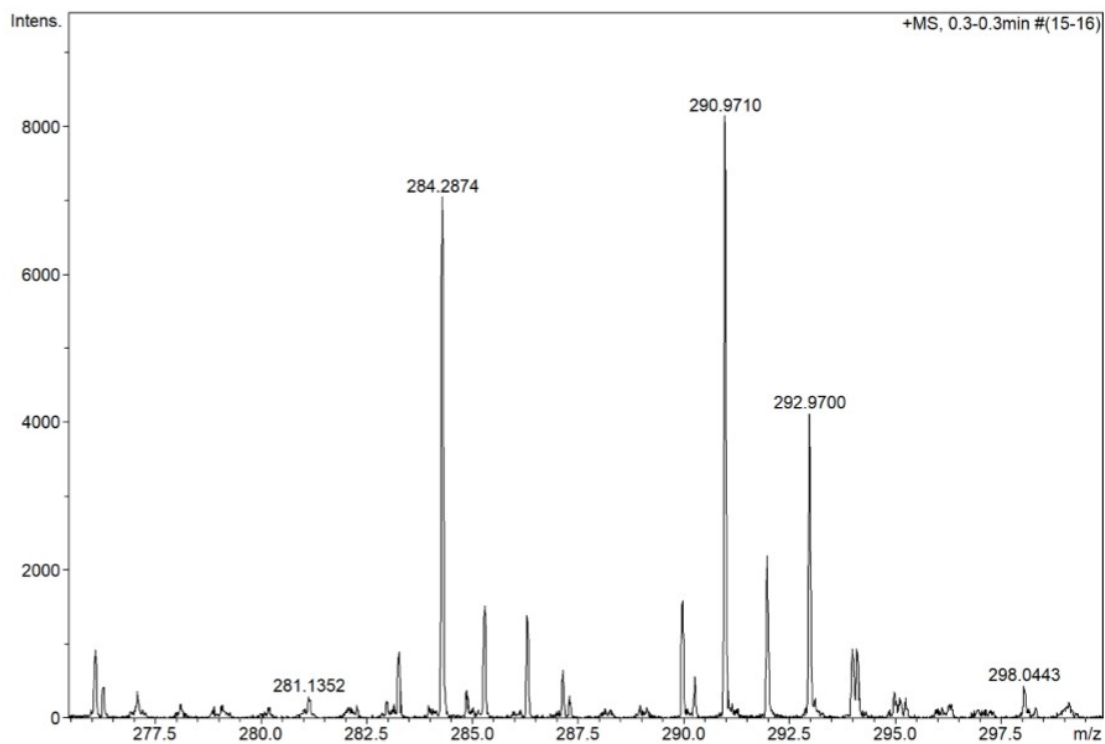


Fig. S44. ESI-MS of SZn.

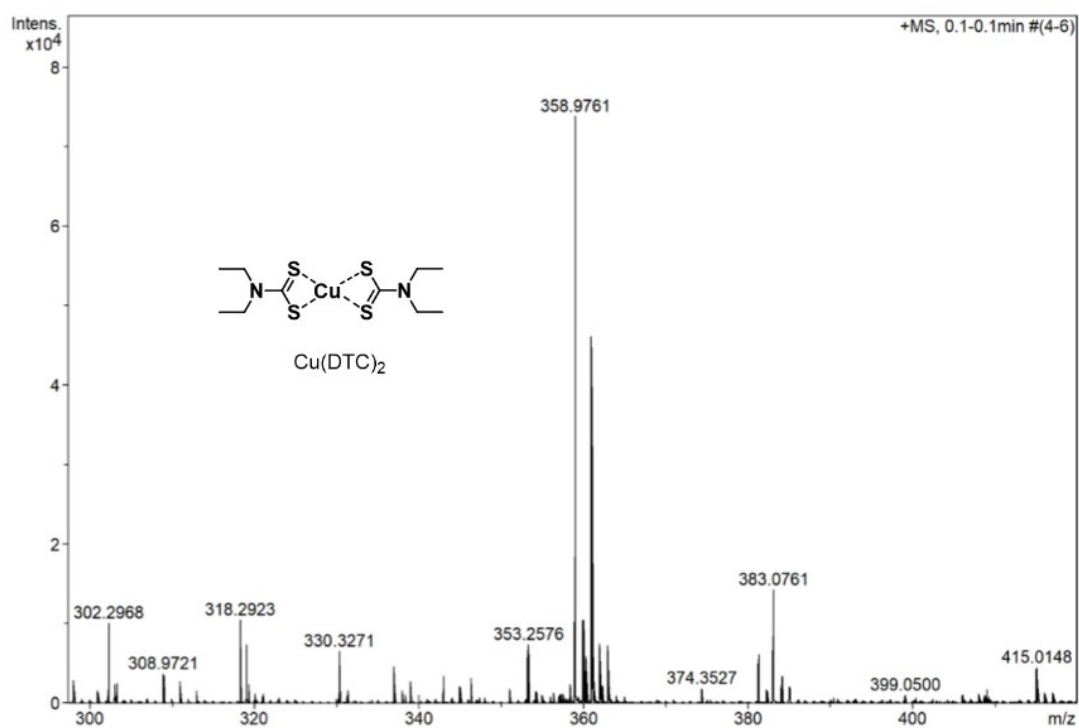


Fig. S45. ESI-MS of Cu(DTC)₂.

Supporting Tables

Table S1. Inhibitory activity (IC_{50} , μM) of DSF and all analogues against four M β Ls.

IC_{50} (μM)	NDM-1 (B1)	IMP-1 (B1)	ImiS (B2)	L1 (B3)
DSF	0.13 \pm 0.05	2.9 \pm 0.8	3.6 \pm 0.7	-
3a	0.26 \pm 0.03	0.53 \pm 0.22	1.8 \pm 0.4	-
3b	0.14 \pm 0.06	0.88 \pm 0.34	0.49 \pm 0.24	-
3c	0.12 \pm 0.05	0.95 \pm 0.32	3.7 \pm 1.2	-
3d	0.32 \pm 0.03	1.7 \pm 0.6	2.6 \pm 0.7	-
3e	0.22 \pm 0.08	0.57 \pm 0.08	0.9 \pm 0.3	-

Note: -, >20 μM

Table S2. Inhibitory activity (IC_{50} , nM) of copper complexes of all DSF analogues against four M β Ls.

IC_{50} (nM)	NDM-1 (B1)	IMP-1 (B1)	ImiS (B2)	L1 (B3)
Cu(DTC) ₂	3.9 \pm 1.6	12.5 \pm 3.8	38.9 \pm 11.3	-
3a-Cu	7.2 \pm 3.2	18.6 \pm 4.6	36.2 \pm 8.6	-
3b-Cu	5.3 \pm 2.6	19.4 \pm 6.4	63.5 \pm 13.6	-
3c-Cu	4.9 \pm 1.5	22.5 \pm 5.8	48.7 \pm 12.5	-
3d-Cu	5.4 \pm 2.8	11.3 \pm 4.6	77.5 \pm 12.5	-
3e-Cu	7.5 \pm 3.4	15.6 \pm 7.2	59.4 \pm 15.2	-

Note: "-" no inhibition (>20 μM inhibitor).

Table S3. Antibacterial activities (MICs, $\mu\text{g}/\text{mL}$) of imipenem against different *E. coli* strains expressing NDM-1, IMP-1 and ImiS in the presence and absence of DSF analogues at 16 $\mu\text{g}/\text{mL}$, respectively.

Compds	<i>E. coli</i> -NDM-1	<i>E. coli</i> -IMP-1	<i>E. coli</i> -ImiS
IMI alone	128	64	64
DSF	16	16	8
3a	16	8	16
3b	8	8	16
3c	4	4	16
3d	32	16	32

3e	8	8	8
----	---	---	---

Table S4. MIC ($\mu\text{g/mL}$) of imipenem against clinical strains producing NDM-1 in the presence of inhibitor at 16 $\mu\text{g/mL}$.

	EC01	EC06	EC10	EC24	<i>K. pneumoniae</i> (NDM-1)	<i>P. aeruginosa</i> (NDM-1)
Control	64	128	64	64	128	64
DSF	8	16	8	16	16	32
Cu(DTC) ₂	4	8	2	16	8	16

Note: EC01-24: clinically isolates *E. coli* producing NDM-1.

Table S5. Multiple in MIC ($\mu\text{g/mL}$) of imipenem against *E. coli* expressing NDM-1 and clinical strains producing NDM-1 at a DSF concentration range of 1–64 $\mu\text{g/mL}$.

Strains	Control	+1 $\mu\text{g/mL}$	+4 $\mu\text{g/mL}$	+16 $\mu\text{g/mL}$	+64 $\mu\text{g/mL}$
<i>E. coli</i> - NDM-1	128	128	64	16	2
EC01	64	64	32	8	4
EC10	64	128	64	32	4

Table S6. Antibacterial activities (MICs, $\mu\text{g/mL}$) of imipenem (IMI) against different *E. coli* strains expressing NDM-1, IMP-1 and lmiS in the presence and absence of Cu(DTC)₂ analogues at 16 $\mu\text{g/mL}$, respectively.

Compds	<i>E. coli</i> -NDM-1	<i>E. coli</i> -IMP-1	<i>E. coli</i> -lmiS
IMI alone	128	64	64
CuCl ₂	>128	>128	>128
Cu(DTC) ₂	8	8	4
3a-Cu	8	4	8
3b-Cu	4	8	8
3c-Cu	4	4	16
3d-Cu	16	8	16
3e-Cu	4	4	4

Table S7. MICs of imipenem against *E. coli*-NDM-1, *E. coli*-C208A-NDM-1 and *E. coli*-L1.

	<i>E. coli</i> -NDM-1	<i>E. coli</i> -C208A-NDM-1	<i>E. coli</i> -L1
Control	128	0.25	32
DSF	16	0.25	32
Cu(DTC) ₂	8	0.25	32

Note: a concentration of inhibitor 16 µg/mL.

Table S8. Cu(DTC)₂ circumvent the reduction by the against *E. coli*-NDM-1.

Strain	Blank (IMI)	+ Cu(DTC) ₂	+β-ME	+Cu(DTC) ₂ and β-ME	+Cu(DTC) ₂ and DTT	+Cu(DTC) ₂ and Cys
<i>E.coli</i> -NDM-1	128	8	256	16	16	8

Note: a concentration of inhibitor 16 µg/mL, Imipenem (IMI).

Table S9. Primer sequenceSs (5'-3')

Primer name	Primer sequence
NDM-1_Ndel_F	5' ATA CAT ATG CAG CAA ATG GAA ACT3'
NDM-1_XhoI_R	5' CGG CTC GAG AGC GCA GCT TGT CGG 3'
NDM-1_C208A_FS	5' GGT GGC GCC CTG ATC AAG 3'
NDM-1_C208A_R	5' CTT GAT CAG GGC GCC ACC 3'

Table S10. MICs of imipenem against *E. coli*-BL21, *E. coli*-BL21-MBLs and clinical isolates expressing NDM-1 (EC01-24, *K. pneumoniae*, *P. aeruginosa*).

Strains	MIC (imipenem)	Susceptibility
<i>E. coli</i> -BL21	0.12	sensitive
<i>E. coli</i> -NDM-1-BL21	128	resistant
<i>E. coli</i> -IMP-1-BL21	32	resistant
<i>E. coli</i> -ImiS-BL21	64	resistant
<i>E. coli</i> -L1-BL21	32	resistant
<i>E. coli</i> -C208A-NDM-1	0.25	sensitive
EC01 (NDM-1)	128	resistant
EC04 (NDM-1)	128	resistant
EC06 (NDM-1)	64	resistant
EC08 (NDM-1)	128	resistant
EC10 (NDM-1)	128	resistant
EC24 (NDM-1)	64	resistant
<i>K. pneumoniae</i> (NDM-1)	128	resistant
<i>P. aeruginosa</i> (NDM-1)	64	resistant